A COMPARATIVE EVALUATION OF SUPER – RESOLUTION METHODS ON COLOR IMAGES

A THESIS SUBMITTED TO
THE GRADUATE SCHOOL OF NATURAL AND APPLIED SCIENCES
OF
MIDDLE EAST TECHNICAL UNIVERSITY

BY

FULYA ERBAY

IN PARTIAL FULFILLMENT OF THE REQUIREMENTS
FOR
THE DEGREE OF MASTER OF SCIENCE
IN
ELECTRICAL AND ELECTRONICS ENGINEERING

MAY 2011

Approval of the thesis

A COMPARATIVE EVALUATION OF SUPER – RESOLUTION METHODS ON COLOR IMAGES

submitted by **FULYA ERBAY** in partial fulfillment of the requirements for the degree of **Master of Science in Electrical and Electronics Engineering Department, Middle East Technical University** by,

Prof. Dr. Canan Özgen ___________
Dean, Graduate School of **Natural and Applied Sciences**

Prof. Dr. İsmet Erkmen ___________
Head of Department, **Electrical and Electronics Engineering**

Prof. Dr. Gözde Bozdağı Akar ___________
Supervisor, **Electrical and Electronics Engineering Dept., METU**

Examining Committee Members:

Asst. Prof. Dr. Alptekin TEMİZEL ______________________
Graduate School of Informatics, METU

Prof. Dr. Gözde B. AKAR ______________________
Electrical and Electronics Engineering Dept., METU

Assoc. Prof. Dr. Çağatay CANDAN ______________________
Electrical and Electronics Engineering Dept., METU

Dr. Fatih KAMIŞLI ______________________
Electrical and Electronics Engineering Dept., METU

Dr. L. Murat GEVREKÇİ ______________________
MGEO, ASELSAN

Date: 10.05.2011

I hereby declare that all information in this document has been obtained and presented in accordance with academic rules and ethical conduct. I also declare that, as required by these rules and conduct, I have fully cited and referenced all material and results that are not original to this work.

Name, Last name : Fulya Erbay

Signature :

ABSTRACT

A COMPARATIVE EVALUATION OF SUPER – RESOLUTION METHODS ON COLOR IMAGES

Erbay, Fulya
M.Sc., Department of Electrical and Electronics Engineering
Supervisor: Prof. Dr. Gözde B. Akar

May 2011, 80 pages

In this thesis, it is proposed to get the high definition color images by using super – resolution algorithms. Resolution enhancement of RGB, HSV and YIQ color domain images is presented. In this study, three solution methods are presented to improve the resolution of HSV color domain images. These solution methods are suggested to beat the color artifacts on super resolution image and decrease the computational complexity in HSV domain applications. PSNR values are measured and compared with the results of other two color domain experiments. In RGB color space, super – resolution algorithms are applied three color channels (R, G, B) separately and PSNR values are measured. In YIQ color domain, only Y channel is processed with super resolution algorithms because Y channel is luminance component of the image and it is the most important channel to improve the resolution of the image in YIQ color domain. Also, the third solution method suggested for HSV color domain offers applying super resolution algorithm to only value channel. Hence, value channel carry brightness data of the image. The results are compared with the YIQ color domain experiments. During the experiments, four different super resolution algorithms are used that are Direct Addition, MAP, POCS and IBP. Although, these methods are widely used reconstruction of monochrome images, here they are used

for resolution enhancement of color images. Color super resolution performances of these algorithms are tested.

Keywords: Color Super - Resolution, Color Image Reconstruction, Image Enhancement in HSV Color Domain, Hue Channel Regularization, Image Enhancement, Image Reconstruction

ÖZ

SÜPER CÖZÜNÜRLÜK METODLARININ RENKLİ GÖRÜNTÜLER ÜZERİNDE KARŞILAŞTIRMALI DEĞERLENDİRMESİ

Erbay, Fulya
Yüksek Lisans, Elektrik Elektronik Mühendisliği Bölümü
Tez Yöneticisi: Prof. Dr. Gözde B. Akar

Mayıs 2011, 80 sayfa

Bu tezde, renkli görüntüler üzerinde süper çözünürlük algoritmaları uygulanmıştır. RGB, HSV ve YIQ renk uzaylarındaki görüntülerin çözünürlüğü arttırılmıştır. Bu tezde HSV renk uzayındaki görüntülerin iyileştirilebilmesi için üç çözüm metodu önerilmiştir. Bu çözüm önerileri HSV renk uzayındaki süper çözünürlüklü görüntülerin üstünde oluşan renk bozulmalarını gidermeyi ve işlem yükünü azaltmayı amaçlamaktadır. Bu renk uzayında elde edilen PSNR değerleri, diğer iki renk uzayından elde edilen sonuçlarla karşılaştırılmıştır. RGB renk uzayındaki deneylerde görüntünün üç ayrı kanalına süper çözünürlük yöntemleri uygulanarak PNSR ölçümleri alınmıştır. YIQ renk uzayında yapılan çalışmalarda, sadece Y kanalına süper çözünürlük algoritmaları uygulanmıştır. Y kanalı, YIQ renk uzayındaki görüntünün aydınlık bileşenidir bu nedenle görüntünün çözünürlüğünü arttırmak için Y kanalının çözünürlüğünü arttırmak çok önemlidir. HSV renk uzayı için önerilen üçüncü yöntemde de benzer şekilde V (parlaklık) kanalına süper çözünürlük algoritmaları uygulanmıştır. Elde edilen sonuçlar, YIQ renk uzayındaki çalışmalardan elde edilen sonuçlarla karşılaştırılmıştır. Yapılan deneyler sırasında dört farklı süper çözünürlük algoritması kullanılmıştır. Bu algoritmalar genellikle

siyah beyaz görüntülerin çözünürlüğünü arttırmak için kullanılır ancak bu tezde bu algoritmaların renkli görüntüler üzerindeki performansları da test edilmiştir.

Anahtar Kelimeler: Renkli Görüntülerde Süper – Çözünürlük, Renkli Görüntülerde Yapılandırma, HSV Renk Uzayında Görüntü İyileştirme, Hue Kanalında Düzenleme, Görüntü İyileştirmesi, Görüntü Yapılandırması.

to my beloved family

ACKNOWLEDGEMENTS

I wish to express my deepest thanksgiving to my supervisor, Prof. Dr. Gözde Bozdağı Akar for her boundless help, excellent supervision and leading guidance from beginning to end of thesis work.

I would like to express my greatest thanks to my parents, Cemile Erbay and H. İbrahim Erbay for their never ending supports their devotion to my overall education, their deep faith in me and in this thesis. I am forever grateful to them for their understanding, endless patience, love, caring and encouragement and to my brother Ahmet Can Erbay for his love and encouragement.

I wish to thank to my friends, who never stop their encouragement and always continue to motivate me, to all of them but especially to İrem Aydın.

I also express my sincere gratitude to my managers and my colleagues from ASELSAN INC. and ASELSAN INC. itself, for their initiative ideas and guidance that helped to construct this work.

TABLE OF CONTENTS

LIST OF FIGURES

FIGURES

LIST OF TABLES

LIST OF ABBREVIATONS

SR	: Super Resolution
RGB	: Red Green Blue
HVS	: Hue Value Saturation
YCbCr	: Luma, blue-difference and red-difference chroma components.
MAP	: Maximum A-Posteriori
ML	: Maximum Likelihood
MISO	: Multiple Input Single Output
MIMO	: Multiple Input Multiple Output
CFA	: Color Filter Array
NNI	: Nearest Neighbor Interpolation
HR	: High Resolution
DA	: Direct Addition
POCS	: Projection onto Convex Sets
IBP	: Iterative Back Projection
PSNR	: Peak Signal-to-Noise Ratio
CT	: Tomography
MRI	: Magnetic resonance imaging

CHAPTER 1

INTRODUCTION

High resolution images are required in most of the electronic imaging applications. Image quality improvement, especially high resolution image reconstruction becomes important day by day in several areas such as medical imaging, security, satellite imaging, broadcast industry, etc [3]. High resolution images are very useful for medicine to make the right decisions about the diagnosis. Recognizing more details on the x-ray films, tomography and magnetic resonance imaging give better results about the diseases. Also, high resolution satellite images give more details about the area and it is easy to identify an object from similar ones. Image enhancement is a critical component of surveillance and reconnaissance applications. More detailed images are helpful for vehicle identification or license plate recognition in traffic monitoring.

Image capturing environment has sensor and optical limitations. So, there are several hardware techniques that can be used to increase the spatial pixel density [4, 49]. First technique is to reduce the pixel size or increase the number of pixels per unit area in the image. This is called sensor producing technique. Disadvantages of this technique are, it decreases light on the pixel and the quality of the image falls off. Second approach to increase the spatial resolution is to increase the chip size which requires higher capacitance. This approach slows the transfer rate of the charge. So it is an inefficient method. Improving the sensor and optic manufacturing technique is another method of getting high resolution image. As the more advanced sensors or optics are used, more detailed images. Actually, this is an expensive method because it is necessary to change the fabrication technology to beat the physical limitations of the sensors which makes the technology infeasible due to manufacturing costs.

Beside hardware methods, there is software method that can be used to improve the image quality [4, 49]. It is to increase the spatial resolution of the images by using the signal processing techniques which is preferable compared to the aforementioned hardware approaches. Super - Resolution (SR) is one of these methods. The main idea behind super resolution is to fuse the multiple low resolution images into an image to get high resolved image. Low resolution images are noisy, blurred and down sampled images of the same scene taken from different points of views. These low resolution images show different view of the same sight. The important thing is to get the sub pixel information from the low resolved images. By up sampling and shifting the low resolution images new pixel values are found. These new pixel values are combined with the existing ones to construct high resolution image.

Sub pixel shift of low resolution images has to be different from each other. If the pixels are shifted by the integer values, then each low resolved image contain the same information and they will be the shifted version of the same image. Thus, to obtain a high resolution image different sub pixel shifts and aliasing are needed.

Due to the optical limitations imaging-environment is not ideal. During the imaging pipeline, distortions are occurred on low resolution images. So blurred, noisy and aliased low resolution captures can be obtained. Although the main aim of super resolution is to construct a high resolution image from the multiple low resolved images, image reconstruction and image enhancement techniques has to be concerned [4].

First formulation of obtaining high resolved image from multiple low resolution, displaced images was considered by Tsai and Huang in 1984 [1]. They utilized the shift property of Fourier transform in their study. They formulated the problem in frequency domain. In 1992, Tekalp, Ozkan and Sezan added the point spread function of the imaging system and observation noise to their equations [2].

Super Resolution Methods can be categorized into two groups such as Frequency Domain Methods and Spatial Domain Methods:

Spatial- Domain Super resolution Methods:

- Interpolation of Nonuniformly-Spaced Samples [18, 19, 20, 21, 22]
- Algebraic Filtered Back-Projection Methods [23]
- Iterative Back-Projection Methods [24, 7, 25, 26]
- Stochastic Methods [27, 28]
- Set Theoretic Methods [2, 29, 30, 31]
- Hybrid Methods [32, 33]
- Optimal and Adaptive Filtering Methods [34, 35]

Frequency- Domain Super resolution Methods:

- Restoration via Alias Removal [1, 36]
- Recursive Least Squares Methods [37, 38, 39]
- Recursive Total Least Squares Methods [3]
- Multichannel Sampling Theorem Methods [40, 41]

These methods will be explained in detail in chapter 2.

1.1 Scope of the Thesis

In this thesis, super resolution performance is analyzed in several color domains using well known reconstruction techniques. The aim of the thesis is to compare the performance of super resolution algorithms in different color domains in terms of quality and computational complexity. Registration parameters are assumed to be known for the sake of argument.

MATLAB is used to implement the algorithms. The Nearest Neighborhood, Bilinear and Bicubic Interpolation methods, Direct Addition, Maximum A-Posteriori (MAP) estimation, Projection onto Convex Sets and Iterative Back Projection algorithms implemented by software. Low resolution images are shifted, deblurred and up sampled by image processing techniques. Finally the PSNR values are presented to demonstrate the success of the proposed super-resolution techniques in specific color domain. We believe that this thesis is valuable to provide inside to super-resolution formation in color domain along with the computational load analysis of each method.

1.2 Thesis Outline

This thesis is composed of five chapters. Brief information about Super Resolution is given in chapter 1.

In Chapter 2, Super Resolution algorithms are examined in details. Also, literature survey has introduced in this chapter. Super resolution approach and observation model are given. Also, basic image interpolation and image registration methods explained shortly.

In Chapter 3, the suggested solution methods for HSV color domain are introduced in details. Implementations of four super resolution algorithms in RGB, HSV and YIQ color domains are given. Besides the detailed methods, example images are shown in this chapter as well. Also, color artifacts that occur in hue channel are examined properly.

In Chapter 4, implementations and results are given about our work.

In Chapter 5, a conclusion is drawn and possible future studies are discussed.

CHAPTER 2

SUPER RESOLUTION METHODOLOGY

First of all, we start this chapter by the mathematical formulation of the super resolution. Methodology of super resolution is discussed in details. Application of monochrome super resolution algorithms to color channels separately to color images is elaborated. Also, difficulties in color image super resolution are presented.

2.1 The Formal Definition

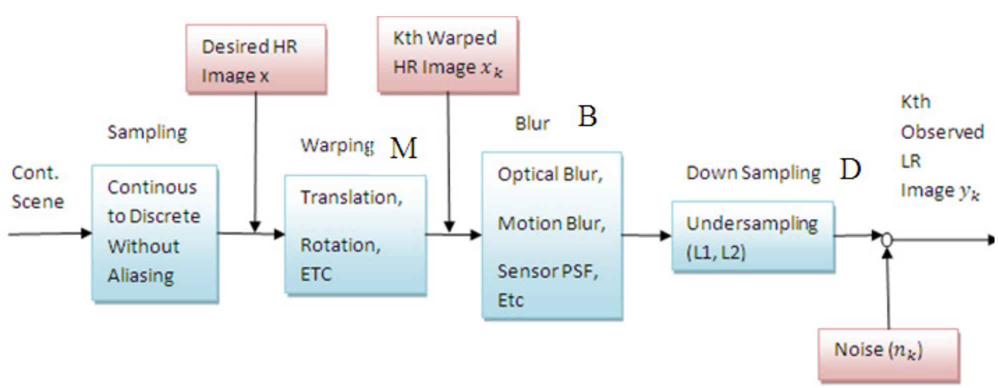

Figure 1. Observation Model

In the literature, there are several observation models for super resolution formation. They are divided into two groups for still images and for video sequences. The basic one is the observation model of SR reconstruction techniques for still images. This observation model is given in Figure 1 [4]. Still observation system has multiple frame input and single output image that has a higher resolution. Still image formation is denoted as this multiple Input Single Output (MISO). This observation model can be generalized to SR reconstruction techniques for video sequences. Herein, there are low resolution video sequences as an input and high resolution video sequences as an output. This model is called as Multiple Input Multiple Output (MIMO). So, here we will first start by the former one.

In still observation model, desired HR image can be shown as the vector notation (lexicographical notation) $\mathbf{x} = [x_1, x_2, \dots, x_N]^T$ where N $= L_1 N_1 L_2 N_2$ N is the number of SR pixels. $\mathbf{x}$ is the desired high resolution image of the desired scene. Its size is $L_1 N_1 L_2 N_2 \times 1$. High resolution image is sampled at or above Nyquist rate, it is anti-aliased image. L_1 and L_2 represents the down sampling factors horizontally and vertically, respectively. kth low resolution image can be shown as vector notation (lexicographical notation), $\boldsymbol{y}_k = [y_{k,1}, y_{k,2}, \dots . y_{k,M}]^T$ where $k = 1,2, \dots p$ and $M = N_1 N_2$. M is the number of LR pixels. Each low resolution image size is $N_1 N_2 \times 1$.

In this model, it is assumed that there is no local motion in the scene. All low resolution images monitor the same scene**.** Also by adding the additive noise $\boldsymbol{n}_k$ (noise vector), observation model becomes as follow in Equation (1),

$$\boldsymbol{y}_k = \boldsymbol{D}\boldsymbol{B}_k \boldsymbol{M}_k \mathbf{x} + \boldsymbol{n}_k \text{ ,} \quad \text{where} \quad 1 \leq k \leq p \tag{1}$$

- $\boldsymbol{M}_k$**,** warp matrix, size **:** $L_1N_1L_2N_2 \times L_1N_1L_2N_2$
- $\boldsymbol{B}_k$**,** blur matrix, size : $L_1N_1L_2N_2 \times L_1N_1L_2N_2$
- $\boldsymbol{D}$**,** down sampling matrix, size **:** $(N_1N_2) \times L_1N_1L_2N_2$

Simply observation model can be expressed as in Equation (2).

$$\boldsymbol{y}_k = \boldsymbol{W_k x} + \boldsymbol{n}_k \tag{2}$$

$\boldsymbol{W_k}$ is multiplication of blurring, motion and down sampling matrices and its size is $(N_1N_2) \times L_1N_1L_2N_2$

The above equation set (2) can be extended to vector notation as follows,

$$\begin{bmatrix} Y_1 \\ Y_2 \\ \vdots \\ Y_p \end{bmatrix} = \begin{bmatrix} W_1 \\ W_2 \\ \vdots \\ W_p \end{bmatrix} X + \begin{bmatrix} N_1 \\ N_2 \\ \vdots \\ N_p \end{bmatrix} \tag{3}$$

If the above equation set is tried to solve in minimum least square sense, the following cost function (Equation 4) has to be minimized.

$$Cost = \|\bar{W}X - \bar{Y}\|_2^2 \tag{4}$$

2.2 Super Resolution Approach

Based on still image observation model which is stated in Equation 2, super resolution approach aims to estimate high resolution image **x**, from the given low resolution images $\boldsymbol{y}_k$ for $k = 1,\ldots,p$. Size of observed low resolution images is $N_1 \times N_2$, and size of super resolution image is $L_1N_1 \times L_2N_2$.

2.2.1 Single Frame Resolution Enhancement

Single frame resolution enhancement means to extend the size of image by estimating the lost pixel values from the neighboring pixels. $\boldsymbol{y}_1$ low resolution image is enlarged in single frame resolution enhancement which is the reference low resolution image. In the literature, many interpolation techniques are used to increase the size of the image. By using interpolation techniques it is possible to expand the image pixel density but it is not possible to recover the information loss due to missing pixels.

2.2.1.1 Nearest Neighbor Interpolation

Nearest-neighbor interpolation is one of the basic algorithms of interpolation. As its name implies, nearest neighbor interpolation method selects the nearest pixel values for approximating the non-given pixel value in the image. The nearest pixel value is assigned to the missing pixel values by the kernel in Equation 5 [50]. Also it does not concern the values of other neighboring points at all. After interpolating the image with this method, image quality is affected negatively. Such as, mosaicing effect is occurred on the image and image's visual quality is degraded.

$$h(x) = \begin{cases} 1 & 0 \leq |x| \leq 0.5 \\ 0 & 0.5 \leq |x| \end{cases} \tag{5}$$

2.2.1.2 Bilinear Interpolation

In image processing environment, bilinear interpolation is one of the basic resampling techniques. Bilinear interpolation is straightforward but competent algorithm. As opposed to nearest neighbor interpolation, bilinear interpolation reduces the visual distortions caused by resizing an image to a non – integral zoom factor. Bilinear interpolation gives smoother results than nearest neighbor interpolation. Main point is to fill the bilinear surface with the existing points. HR grid is filled with existing pixel values and zeros are placed between the existing pixel values. Lost pixel information is estimated by using the 4 nearest pixel values which are located in diagonal direction. This process is repeated until all lost pixel values are calculated and leaving non empty pixel information in the image. The kernel is shown in Equation 6. [50]

$$h(x) = \begin{cases} 1 - |x| & 0 \le |x| \le 1 \\ 0 & 1 \le |x| \end{cases} \tag{6}$$

2.2.1.3 Bicubic Interpolation

Bicubic Interpolation is an advance interpolation method with respect to nearest neighbor and bilinear interpolation. In this method, 4 by 4 pixels are used for estimating the missing pixel values in the high resolution image grid. Bicubic interpolation uses a polynomial passing through four pixels to make a decision. The result image is smoother and has higher quality than bilinear and nearest neighbor interpolation. Equation 7 shows the bicubic interpolation formula [50]. It has to be applied both row and column of an image. This equation is the continuous time convolution kernel of the cubic interpolation.

$$h(t) = \begin{cases} \frac{3}{2}|t|^3 - \frac{5}{2}|t|^2 + 1 & 0 \leq |t| \leq 1 \\ -\frac{1}{2}|t|^3 + \frac{5}{2}|t|^2 - 4|t| + 2 & 1 \leq |t| \leq 2 \\ 0 & |t| > 2 \end{cases} \tag{7}$$

2.2.2 Multi – Frame Resolution Enhancement

Lost pixel value can be estimated due to distribution function of the image but single frame interpolation techniques are inadequate to get the high frequency components after down sampling of the image due. Mainly, the goal is to get more details of the imaging scene to improve the resolution of the image. For this purpose, more pixel values and different scene information is needed. Because of this reason, new methods are issues of the researchers. Super Resolution approach correspond the main demand. Super resolution methods are the second-generation technique of image restoration that is understood to mean bandwidth extrapolation beyond the diffraction limit of the optical system [3].

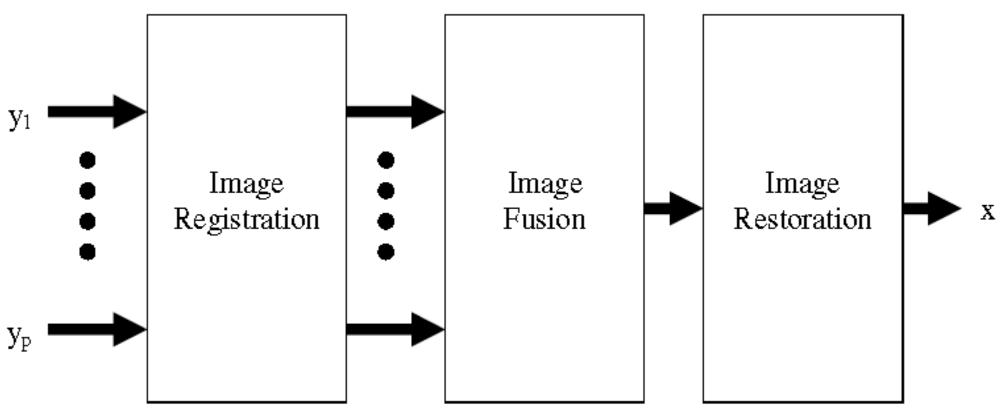

Figure 2. Super resolution pipeline

Super Resolution methods consist of two main parts. First part is to align the low resolved images for getting the pixel information for every pixel to the position of reference; second part is combining the information bits about the original pixel value and to recover the missing pixels of the high resolved image by restoration. In Figure 2, three basic steps of super resolution methods are shown. First step is image registration, where low resolution images are registered to reference grid. Second step is image fusion where LR images are fused to a HR image. And last step is image restoration where result image is processed by deblurring and denoising methods. In some super resolution methods these steps are implemented simultaneously.

Sub pixel shift is the most critical part for super resolution algorithm to improve the resolution. This issue determines the accuracy of image registration. If pixel shift is in integer value, the copies of the same image will be obtained. This action gives no extra information to recover the lost information. Subpixel shifts is shown in Figure 3 [4].

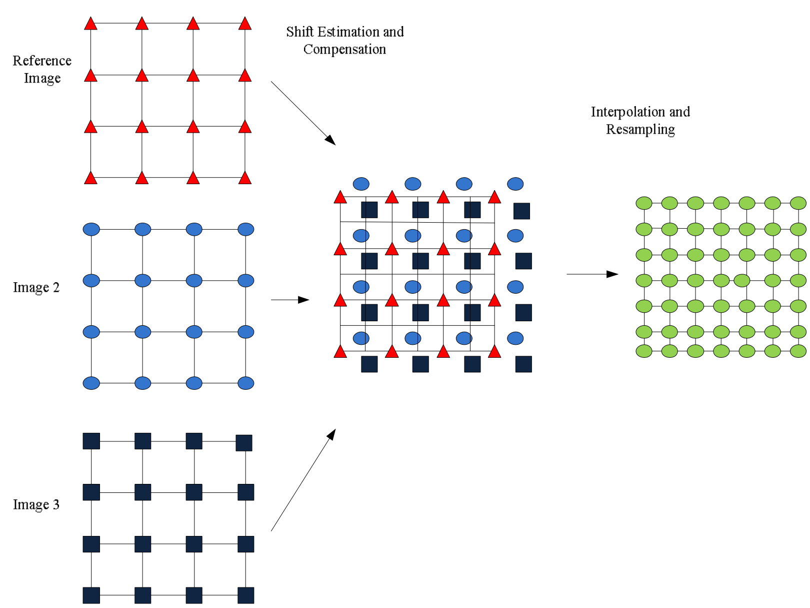

Figure 3. Subpixel Shifts

2.2.2.1 Image Registration

Image registration is the method of aligning multiple images on the same grid. Registering frames of a video or images from a sequence is mainly about solving the problem of geometric relation with the reference image and finding the right way to put them on the same geometrical grid. It is the key step in all image analysis tasks in which the desired information is related to some motion in the picture or the camera. Image registration is extremely important in super-resolution scheme since the artifacts caused by an incorrectly aligned image are more disturbing than the blurring effect caused by interpolation of only one image. Image registration is the process of overlaying images (two or more) of the same scene taken at different times, from different viewpoints, and/or by different sensors. The registration geometrically aligns two images (the reference and sensed images).

There are several different image registration algorithms.

- <u>Optical flow algorithm</u> is an example of non-rigid image registration algorithm. This algorithm is based on estimation of relative motion between images. [42, 52]

- <u>Feature based registration</u> is based on the extraction of the features in the image and finding the corresponding points in other images. Establishing the correspondence allows estimating the homography. [53]

- <u>Phase correlation</u> is based on the Fourier Shift Theorem and was originally proposed for the registration of translated images. It computes the cross-power spectrum of the sensed and reference images and searches for the location of the peak in inverse Fourier domain. [53]

- Template based registration techniques register images of a scene and a model of the scene using region of interest along with selected deformation model. [52]

2.2.2.2 Super Resolution Algorithms

It is stated that, there are two main steps in super resolution concept. The first one is image registration and the later one is image reconstruction step. After the low resolution images are registered, they should be combined in a suitable way.

2.2.2.2.1 Regularized Super Resolution Methods

2.2.2.2.1.1 Maximum A Posteriori Estimation

Super – resolution is an ill – conditioned problem of estimating the high resolution images from the sequence of low resolution images. Bayesian techniques and generic smoothness assumptions about the solution can be used as super resolution method because of the ill – conditioned point of the problem. Problem is ill – conditioned because there is insufficient number of LR images and it is ill – posed due to the blur operators. Regularization procedures are needed to stabilize the inversion of ill – posed problems. In this thesis, it is introduced maximum a posteriori (MAP) SR image reconstruction method as a stochastic regularization approach.

Prior distribution of high resolution image is used to formulate the regularization and the solution is explained with MAP optimization. Prior information is a function interpreting a priori knowledge about probability distribution of estimated signal shape. Bayesian approach provides a convenient and flexible way to model a priori knowledge about the solution. So, stochastic SR image reconstruction is based on Bayesian approach. If one can establish the probability density function (PDF) of the original image, Bayesian methods can be used.

MAP optimization method maximizes the PDF of high resolution image given the low resolution images in Equation 8.

$$x_{MAP} = argmax\left[\frac{\Pr(y_k|x).\Pr(x)}{\Pr(y_k)}\right] \tag{8}$$

Taking the logarithmic function of Equation 8 gives the following statement,

$$x_{MAP} = argmax(\ln[\Pr(y_k|x)] + \ln[\Pr(x)] - \ln\,[\Pr(y_k)])$$

$\ln\,[\Pr(y_k)]$ term can be omitted from the statement since it does not effect the maximization of the statement.

$$x_{MAP} = argmax(\ln[\Pr(y_k|x)] + \ln[\Pr(x)]) \tag{9}$$

MAP solution for the SR problem can be written as in Equation 10.

$$x_{MAP} = argmax\left(\ln\left[\prod_{k=1}^{p} \Pr(y_k|x)\right] + \ln[\Pr(x)]\right) \tag{10}$$

Observation noise is assumed to be zero mean Gaussian distribution and in this case data fidelity term and $\Pr(x)$ term can be expressed as follows,

$$\Pr(y_k|x) = \frac{1}{\sqrt{2\pi}.\sigma}.\exp\left\{-\frac{1}{2\sigma^2}(y_k - DB_kM_kx)^T(y_k - DB_kM_kx)\right\} \tag{11}$$

$$\Pr\,(x) = \frac{1}{\sqrt{2\pi}.\sigma}\exp\left\{-\frac{1}{2}x^TC^{-1}x\right\} \tag{12}$$

By inserting the Equations 11 and 12 into the Equation 10 and taking the logarithm of both sides cost function can be obtained. Cost function (Equation 13) has to be minimized to get the solution.

$$cost = \hat{x} = \underset{x}{\arg min} \left[\sum_{k=1}^{p} \left|\left|DB_k M_k x - y_k\right|\right|_2^2 + \lambda \|Cx\|_2^2\right] \quad (13)$$

$\sum_{k=1}^{p} \left|\left|DB_k M_k x - y_k\right|\right|_2^2$, data fidelity term.

$\lambda \|Cx\|_2^2$, smoothness parameter.

C: High Frequency Filter Function. Generally, C is designed as spatial difference and the norm function that belongs to that spatial difference.

λ: Regularization parameter. λ satisfies the trade of between the smoothness factor and the data fidelity. Large values of λ leads to the smoother results. This case is useful when there is small number of low resolution images. If there is large number of LR images and the observation noise is small then small λ will lead to good results.

Taking the derivative of the cost function with respect to *x* and setting the derivative to zero gives the minimum solution.

$$\nabla cost = \sum_{k=1}^{p} 2(M_K B_K D)^T (DB_K M_K x - y_k) + 2\lambda C^T C x \quad (14)$$

Cost function can be expressed iteratively using steepest descent algorithm as follows,

$$x^{n+1} = x^n - \beta . \nabla cost$$

By substituting $\nabla cost$, Equation 15 can be obtained.

$$\hat{x}^{n+1} = \hat{x}^n + \beta\left[\sum_{k=1}^{p} [(M_k^T B_k^T D^T)(y_k - DB_k M_k \hat{x}^n)] - \lambda C^T C \hat{x}^n\right] \quad (15)$$

2.2.2.2.1.2 Maximum Likelihood Estimation

Maximum likelihood estimation (MLE) is another technique that is used as regularized super resolution method in SR reconstruction. It is the special form of MAP estimation technique. If there is no information related to $\ln[\Pr(x)]$ term in Equation 10, this term can be considered to have uniform distribution. Due to its value is zero, solution procedure is not affected by this term. ML estimator relies on the observations and this method investigates the most likely solution to the observed data. Hence ML estimation technique is noise sensitive; MAP estimation technique is preferred in most applications.

Maximum likelihood estimation technique is also based on the Bayesian theorem. Solution procedure is similar to MAP solution, so same steps (Equations 10 to 15) will be followed to obtain the ML solution.

ML solution for the SR problem can be written as in Equation 16.

$$x_{ML} = argmax(\ln\left[\prod_{k=1}^{p} \Pr(y_k|x)\right] \tag{16}$$

Observation noise is assumed to be zero mean Gaussian distribution and in this case data fidelity term can be expressed as follows,

$$\Pr(y_k|x) = \frac{1}{\sqrt{2\pi}.\sigma}.\exp\{-\frac{1}{2\sigma^2}(y_k - DB_kM_kx)^T(y_k - DB_kM_kx)\} \tag{17}$$

By substituting Equation 17 in Equation 16 and taking the logarithm of both sides cost function can be obtained. Cost function (Equation 18) has to be minimized to get the solution.

$$cost = \hat{x} = \underset{x}{\arg min}\,[\textstyle\sum_{k=1}^{p} ||DB_kM_kx - y_k||_2^2] \tag{18}$$

Taking the derivative of the cost function with respect to x and setting the derivative to zero gives the minimum solution.

$$\nabla cost = \sum_{k=1}^{p} 2(M_K B_K D)^T (D B_K M_K x - y_k) \tag{19}$$

ML solution can be obtained as in Equation 20.

$$\widehat{x_{ML}} = [\sum_{k=1}^{p} (M_k^T B_k^T D^T D B_k M_k)]^{-1} . \sum_{k=1}^{p} (M_k^T B_k^T D^T y_k) \tag{20}$$

Cost function can be expressed iteratively using steepest descent algorithm as follows,

$$x^{n+1} = x^n - \beta . \nabla cost$$

By substituting $\nabla cost$, Equation 21 can be obtained.

$$\hat{x}^{n+1} = \hat{x}^n + \beta \sum_{k=1}^{p} [(M_k^T B_k^T D^T)(y_k - D B_k M_k \hat{x}^n)] \tag{21}$$

2.2.2.2.2 Direct Addition

The simplest image reconstruction algorithm is Direct Addition algorithm among monochrome SR algorithms. This method is based on to get mean or median of the images. These two methods are very easy to implement. But Direct Addition algorithm has some drawbacks such as blurring, and distortion of details that are not present in every image. On the other side, this method can reduce the effects of noise and misregistrations (deregistrations) successfully, because mean and median operations have low pass filter characteristic. Also, Direct Addition method allows adding the image restoration methods to the algorithm. In addition to these, the two variants of direct addition methods are single-run methods and have a very low computational complexity.

The direct addition algorithm is very simple and has a few steps, which are independent from image filtering scheme changes. First, observed low resolution images are upsampled by using bilinear or bicubic interpolation. After that these upsampled and aligned images are added to form the final SR image. The type of addition determines the filtering type as median or mean. The mean filtering of upsampled-registered images takes the mean of all overlapping pixel values (Equation 22), whereas the median filtering takes the median value of each overlapping pixel set (Equation 23).

$$HR(x,y) = \sum_{i=1}^{n} \frac{(\uparrow LR)(x,y,i)}{n} \qquad \forall x,y \in HR \tag{22}$$

$$HR(x,y)A = median\big((\uparrow LR)(x,y,n)\big) \qquad \forall x,y \in HR \tag{23}$$

$\uparrow$: upsample the low resolution images.

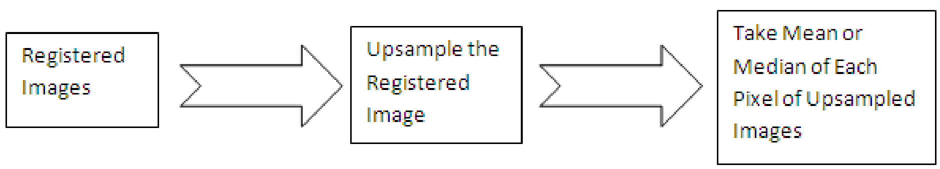

Figure 4. Pipeline of Direct Addition with Median Filtering Algorithm

2.2.2.2.3 Iterative Backprojection

Single – run methods are not good at solving super resolution reconstruction problem. It is possible to increase the performance by using an iterative methodology. Iterative methods use prior information of the previous results to get a better output. Most of the iterative super resolution methods have in common and powerful simulate-and-correct approach to restoration. One of them is the iterative backprojection method. It is very simple to understand in application. The IBP method needs a priori image to start the process [3]. This method uses the mean of the registered images, as the priori image. This image is the base image to reconstruct the SR image. The basic idea of this algorithm is to generate a simulation image, generate LR images from the simulation image to compare them with the observed LR images and using the error between them to generate a better quality simulation. There has to be an ending rule for this algorithm otherwise algorithm repeats the steps continuously. A threshold value or a defined number of iterations may be an ending rule.

The aim of the IBP method is to minimize the error between simulated LR images and the observed LR images iteratively. By taking weighted average of various LR pixels, all corrections on the simulated HR image is generated using the back projection kernel [7].

Algorithm is easy to understand. However, due to the ill-posed characteristic of the problem the solution is not unique. Choice of the base image is very critical part of the algorithm, where the solution may not converge or the solution converges too slowly. In fact, many solutions that satisfy the constraints given by the observed low-resolution frames exist [3].

Iterative backprojection method simulates the forward problem using an initial HR estimate and back projects the error between the simulated and real low resolution images.

$$ysim_k^n = DB_kM_k.\hat{x}^n + n_k \qquad k = 1,..,p \tag{24}$$

$$\hat{\boldsymbol{x}}^{n+1} = \hat{\boldsymbol{x}}^n + \beta[\textstyle\sum_{k=1}^{p} \boldsymbol{h}^{BP}.(\boldsymbol{y}_k - \boldsymbol{ysim}_k^n)] \tag{25}$$

$$\hat{x}^{n+1}[n_1, n_2] = \hat{x}^n[n_1, n_2] + \textstyle\sum_{k=1}^{p} y_k[m_1, m_2] - ysim_k^n[m_1, m_2] \times \boldsymbol{h}^{BP} \tag{26}$$

Where n is the iteration number, $\hat{x}$ is the simulated HR image, p is the number of images, $\boldsymbol{y}_k$ is the observed LR images and $\boldsymbol{ysim}_k^n$ is the final simulation of LR images after n iterations and n1,n2 are the HR space and m1,m2 is the LR space.

Finally, $\boldsymbol{h}^{BP}$ is the backprojection kernel. $\boldsymbol{h}^{BP}$ may be utilized as an additional constraint, which represents the desired property of the solution [3].

2.2.2.2.4 Projection on the Convex Sets (POCS)

The other iterative solution to the SR reconstruction problem is Projection onto Convex Sets (POCS) method. The aim of this algorithm is to minimize the error iteratively as well. POCS method is the most known set theoretic method which solves the restoration problem by defining constraint sets of which must be satisfied by candidate solutions [4]. The convex sets are the observed low resolution data, in our study. POCS method finds alternative solutions for every pixel value, which satisfies the convex sets, simultaneously. Stark and Oskoui [29] use convexity and closeness of the constraint sets. Their aim was to guarantee convergence of iteratively projecting the images onto these sets. Tekalp, Ozkan, and Sezan [2] state a POCS formulation that is more robust.

Like IBP method, POCS algorithm begins with the determination of the priori constraint, which is the reference frame that is within the solution space. The reference frame interpolated to the HR grid and the first estimate is obtained. The iterative process starts here and processes every frame and every pixel to locate the solution.

First, the images are registered, and the motion compensated coordinates are obtained for every pixel. After that, by applying a Gaussian PSF for every pixel, values of these pixels are projected to the HR grid. Then, solution is obtained for every image. The next step is merging these solutions into the intersection of these sets. Every pixel value has the prior information and the obtained value specific to that set. After that the available estimate is stretched to satisfy the solution set. The pixel value is updated at the level of the threshold to match the projected value as close as possible without disturbing the continuity of the solution. At the end of this step, first iteration is completed. The solutions are normalized to the intensity space [0,255] and the next simulated HR image is ready.

$$x^{n+1} = P_m P_{m-1} \dots P_2 P_1 x^n \qquad (27)$$

where x^0 is an arbitrary starting point, and P^i is the projection operator which projects an arbitrary signal x onto the closed, convex sets, C^i. For each pixel within the LR images $y_k[m_1, m_2]$.

$$r^{(x)}[m_1, m_2] = \; y_k[m_1, m_2] - \sum_{n_1, n_2} x[n_1, n_2]\, W_k[m_1, m_2;\; n_1, n_2] \qquad (28)$$

$$C_D^k[m_1, m_2] = \{x[n_1, n_2]\colon |r^{(x)}[m_1, m_2]| \le \delta_k[m_1, m_2]\} \qquad (29)$$

The projection of an arbitrary $x[n_1, n_2]$ onto $C_D^k[m_1, m_2]$ can be defined as:

$$x^{n+1}[n_1, n_2] = x^n[n_1, n_2] + \begin{cases} \frac{r^{(x)}[m_1, m_2] - \delta_k[m_1, m_2] W_k[m_1, m_2;\, n_1, n_2]}{\sum_{p,q} W_k^2[m_1, m_2 p, q]}, & r^{(x)}[m_1, m_2] > \delta_k[m_1, m_2] \\ 0, & \left| r^{(x)}[m_1, m_2] \right| \le \delta_k[m_1, m_2] \\ \frac{(r^{(x)}[m_1, m_2] + \delta_k[m_1, m_2]) W_k[m_1, m_2;\, n_1, n_2]}{\sum_{p,q} W_k^2[m_1, m_2, p, q]}, & r^{(x)}[m_1, m_2] < -\delta_k[m_1, m_2] \end{cases} \qquad (30)$$

Additional constraints after (30) can be added to improve the results [29].

One of the drawbacks of the POCS method is that the solution is not unique. The solution may converge to any member in the intersection set. And due to the pixel wise recovery of the values, the computational complexity is high. Additionally, the method converges very slowly or even may not converge at all.

CHAPTER 3

COLOR SUPER RESOLUTION

3.1 General View of the Color Super Resolution

In the literature, there is very little work about color super resolution problem. Color images are represented by the combination of three monochromatic images. In other words, unlike the monochrome images, color images have three color channels. Generally, color super resolution approach is separating the image into color components in the defined color domain. For example, if the image is in RGB color domain, it is separated into three channels. These are Red, Green and Blue channels. The typical approach is separating the image into color channels and applying the monochromatic SR algorithms to each channel independently. [5, 6] Generally, in this approach, color information is used to increase accuracy of the motion estimation.

Second approach is transforming the problem to a different color space, where luminance channels are easily identified from chrominance channels and SR algorithm is applied only to the luminance channel. At the beginning of the color super resolution studies, RGB color images are converted to YIQ color images. *Irani and Peleg et.al* followed the same method in their studies. [3]. Y component is luminance component of the image. Luminance component represents the brightness of the image. Chrominance components of the image (I, Q) are contained the color information. Also, the details in the luminance component of the image are more sensible than the details in the chrominance component by the human eye. This property shows that major part of the energy is in the luminance component of the image. Because of this, *Irani and Peleg* are applied Iterative Backprojection method to the Y channel and non-uniform interpolation to I and Q channels to get the high resolved image.

Earlier approaches could not fully utilize the correlation across the color bands so another approach is suggested for color super resolution reconstruction. *Farsiu et al*, are used SR and demosaicking algorithms together, in their study. Demosaicking algorithm was applied to the image after the SR algorithm, unlike the past studies [8]. Ideally, in color images each pixel should be formed from three scalar values, each of for one color band. Generally, to reduce the production cost, color filter arrays (CFA) are placed in front of the CCDs. The most famous color filter array pattern is Bayer Filter shown in Figure 11. By this way, each pixel is made sensitive to one color band and the missing values of color bands are predicted. All missing values are synthesized for each pixel by one interpolation method from the neighboring pixel values. This process is named by color demosaicking. [8] Although, *Farsiu et al* used a different color filter array. Every R, G, B pixels of the low resolution images are aligned on a common high resolution image grid considering their spatially positions and translational motions with respect to each other. By the help of this color filter array which has new distribution, incomplete RGB pixels are predicted by maximum a posteriori based super resolution algorithm. By this way, they obtained high resolved images for each color channel.

Ill – posed nature of the demosaicking problem causes to occur color artifacts on the final high resolution image. This results from the correlation across the color bands. In the literature, various single-frame and multi-frame demosaicing methods have been proposed to reduce these color artifacts [44, 45, 46, 47].

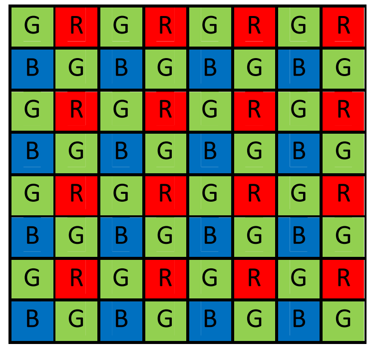

Figure 5. Bayer Pattern. (US Patent 3,971,065, 1976)

3.2 General Color Domains

In this thesis, the three most common color domains are concerned. One of these color spaces is RGB color domain. RGB color domain is called additive color model. Red, Green and Blue light are added together in different ways to get board color array. Primary colors are red, green and blue. The other colors are obtained from these colors. Main purpose of RGB color domain is displaying the images in electronic systems such as computers, televisions [17]. Because human visual system works in a way, that is similar to an RGB color space. Each of R, G, B channels contains color and brightness data of the image and each one has an arbitrary intensity. Hence, all of the color channels have the same priority in color super resolution applications. RGB color space is preferred in SR reconstruction problem among the other color spaces because results are better.

The other color domain is HSV color domain. Mainly, this color domain is also used in color super resolution studies. HSV color space is the most common cylindrical - coordinate representation of RGB color space. RGB to HSV transformation is non-linear but double-faced. As in RGB color space, there are three channels in HSV color space. These are H (hue) channel, S (saturation) channel and V (value) channel. The hue channel represents the colors in their pure form, such as yellow, green and blue. By adding white to the pure color, more saturated color is obtained which is called saturation. The value channel stands for the brightness of the color. Usually, HSV color space is demonstrated by the inverted pyramid. Here, it is showed by Figure 6 [48]. The center of the pyramid represents the value channel of the HSV and it is value is 1 at the top of the pyramid. The hue channel measures the angle around the vertical axis. Due to angular structure of the hue channel, its value changes between $0^{\circ} - 360^{\circ}$. Lastly, value of the saturation channel changes between 0 and 1. It is value is zero at the center of the pyramid and it is one at the surface of the pyramid.

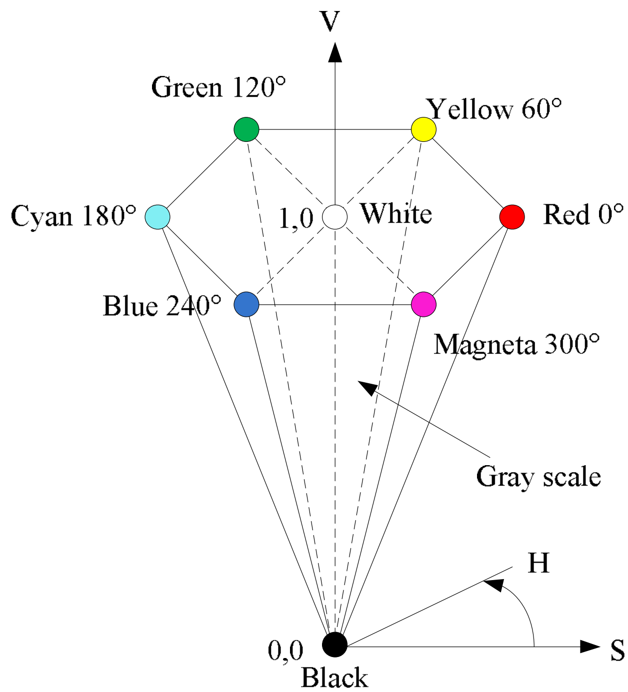

Figure 6. HSV color space representation.

YIQ color space is the last color domain that is used in this thesis. Images in YIQ color domain, are also composed of three channels. These channels are Y, I (in phase) and Q (qudrature). Y is luminance component of the image which contains the black and white information (brightness data) of the image. I, Q are chrominance components that are involved the color information of the image. There is a matrix equation between the RGB and YIQ color spaces. The value of the components can be calculated from the Equation (31).

$$\begin{bmatrix} Y \\ I \\ Q \end{bmatrix} = \begin{bmatrix} 0.299 & 0.587 & 0.114 \\ 0.595716 & -0.274453 & -0.321263 \\ 0.211456 & -0.522591 & 0.311135 \end{bmatrix} \begin{bmatrix} R \\ G \\ B \end{bmatrix} \tag{31}$$

3.3 Color Super Resolution in RGB Color Domain

In this thesis, first color super resolution algorithms are applied to the images that are in RGB color domain. It is obvious that, in RGB color domain all of three channels have the same priority by human eye because additive structure of this color domain is similar to human visual system. In RGB domain, color channels are not separated by luminance component and chrominance component of the light. All of three include color and brightness data of the image, equally. Because of that reason, in RGB domain experiments, color super resolution algorithms are applied to three channels (R, G, B), separately.

As a first step, low resolution images are created from the original image. Blurring, motion and sub sampling steps are followed while creating the low resolution images. The first, reference low resolution image is interpolated by bilinear and bicubic interpolation techniques. After that, super resolution algorithms applied to R, G, B channels of low resolution images to reconstruct a super resolution image. The aim is to distinguish the difference between the interpolation and SR techniques.

3.3.1 Interpolation Techniques Applied to R, G, B Channels

Basically, bilinear and bicubic interpolation methods are used to interpolate the LR image. While constructing the LR images, in motion step, image is moved both in horizontal and vertical direction, randomly. The input low resolution image of the interpolation process is the first and reference image. Reference low resolution image is not displaced any direction because movement of the image cause degradation. Increasing the degradation make results worse. Algorithm flowing chart is given in Figure 7.

Resultant image of interpolation methods are more blurred than super resolution image. Super resolution image is the output of the super resolution methods. As an example, in Figure 9, result images are shown on ‘Lena’ image. Also, enlarged images created by bicubic interpolation are smoother and high quality than interpolated image by bilinear method.

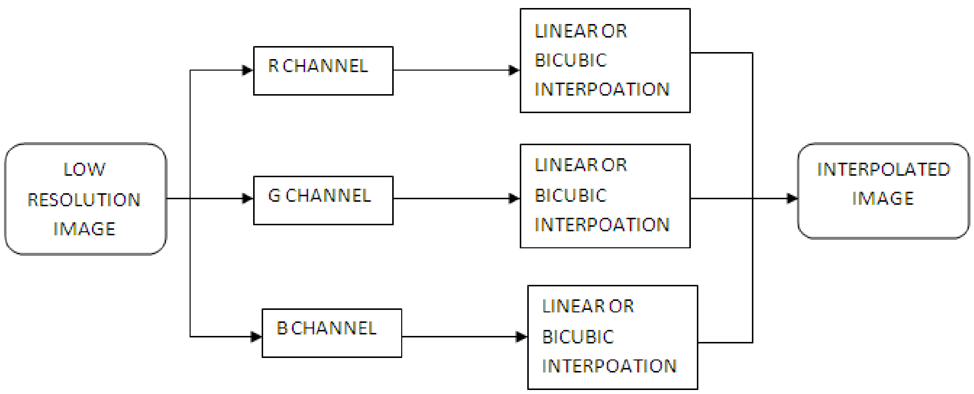

Figure 7. Interpolation Algorithm Flowing Chart

a) b) c)

Figure 8. a) LR Image b) Noisy LR Image c) 512x512 Original Lena Image

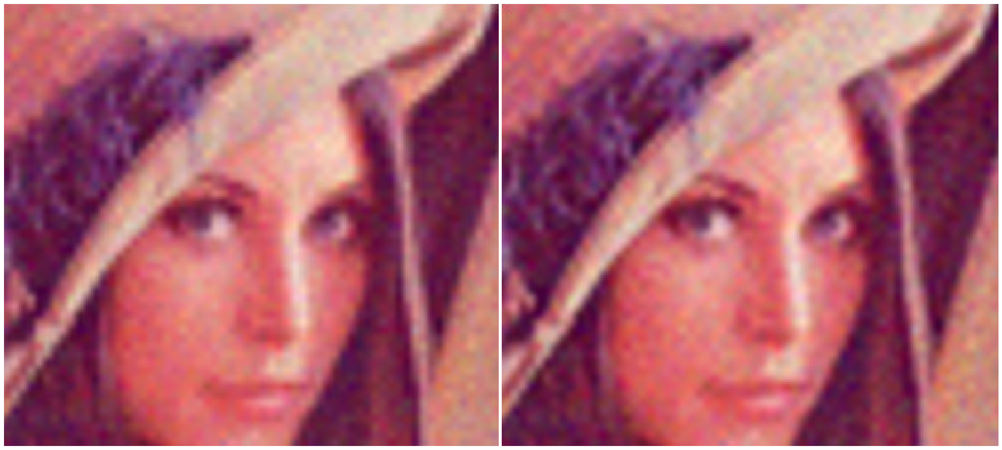

a) b)

Figure 9. a) Bilinear Interpolation b) Bicubic Interpolation.

3.3.2 Super Resolution Techniques Applied to R, G, B Channels

Direct Addition (DA), Maximum A Posteriori (MAP), Projection onto Convex Sets (POCS) and Iterative Back Projection (IBP) super resolution algorithms are applied R, G, B channels and output SR images of each algorithm are compared. In the literature, these methods are widely used in SR reconstruction of monochrome images. In color super resolution, every single color channel can be thought as monochrome image. Therefore, SR algorithms are applied R, G, B channels separately and these images are combined together to obtain the final SR image. Algorithm flowing chart is shown in Figure 10.

MAP, POCS and IBP are the iterative based methods. These algorithms try to minimize the cost function iteratively. Actually, MAP and POCS methods are the special type of the IBP method. Beside this, DA is not an iterative method. It directly shifts and adds low resolution images. Because of this reason, final SR image of DA is more blurred than the others. Visually, MAP and IBP methods have very similar results. Beside this, due to the boundaries used in POCS algorithm, final SR image of POCS is smoother than output of MAP and IBP algorithms. In noisy cases, MAP method gives better results than IBP in RGB domain. High pass filter used in MAP method suppresses the noise and smoother SR image is obtained. If textures are considered in RGB domain color images, IBP method is more successful. If PSNR values are considered, IBP method satisfies the best resemblance to the ground data in RGB color domain. Demonstration of these methods is shown in Figure 11. The detailed results are discussed in chapter 4.

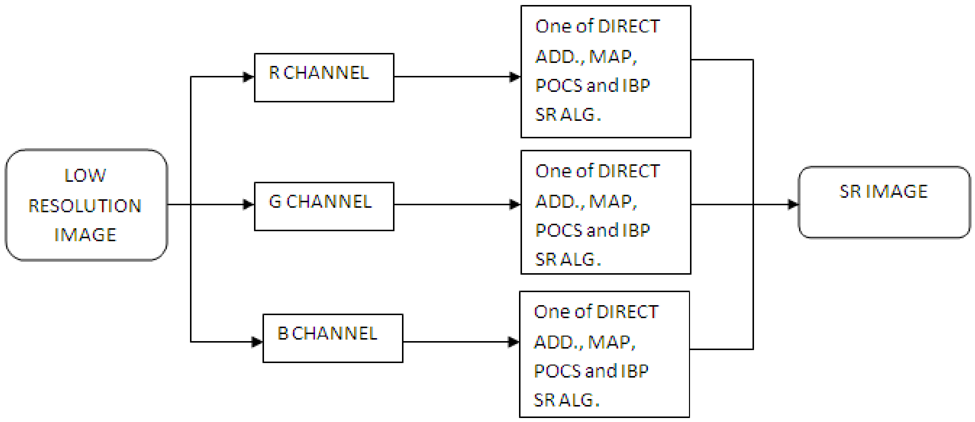

Figure 10. SR Algorithms Flowing Chart

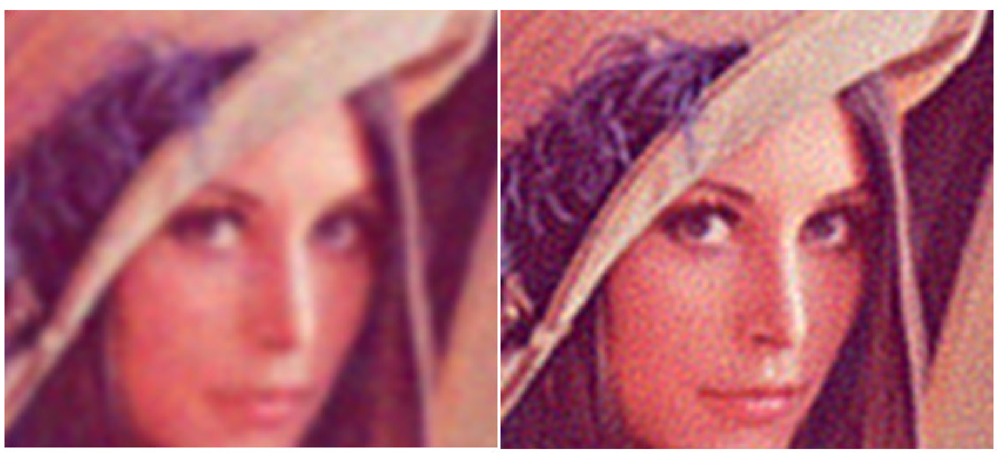

a) b)

c)

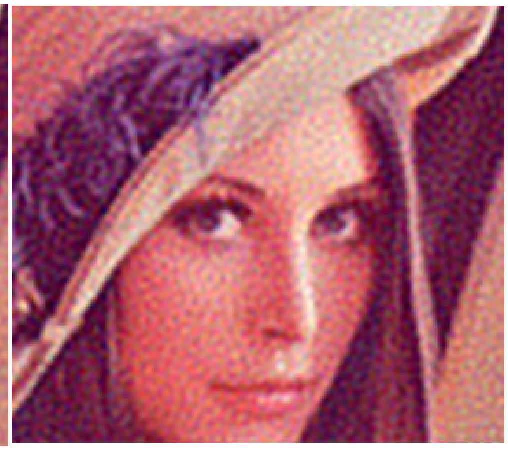

d)

Figure 11. a) DA-RGB b) MAP-RGB c) POCS-RGB b) IBP-RGB

3.4 Color Super Resolution in HSV Color Domain

In this thesis, HSV color domain is the second domain studied on. SR algorithms and interpolation methods that are told before applied to HSV color domain images. If the raw data is in HSV color space, there is no need to transfer the images into another color space such as RGB, YIQ or YCrCb. HSV color space has a special feature. This specialty comes from the angular structure of the hue channel. With the same approach in RGB color domain, original image is separated into H, S and V channels to handle them one by one.

When SR algorithms and interpolation methods are applied to H, S and V channels separately color artifacts are occurred on the both interpolated and SR images. Bilinear and bicubic interpolation methods and DA, MAP, POCS and IBP SR methods are applied to HSV color image, respectively. In Figure 13 and 14, artifacts can be recognized obviously.

This thesis is proposed 3 solution methods to abolish those color artifacts from the super resolution image. The first solution method is applying one of SR algorithms both S and V channels and H channel is treated with a simple interpolation method. The second solution method is Masked – Hue Method. In this method, one of SR algorithms and an interpolation method are applied together to hue channel with mask. The remainder channels are processed by SR algorithm. The last solution method is applying SR algorithm to only Value channel and simple interpolation techniques to H and S channels. These solution methodologies are given in Table 1 and discussed in detail in the next section.

Table 1. Proposed Solution Methodologies in HSV Color Domain

Solution Methods	
HSV1	H Channel => Interpolation, S, V Channels => SR Algorithm
HSV2	H Channel => Masked (SR and Interpolation), S, V Channels=> SR Algorithm
HSV3	H, S Channels => Interpolation, V Channel => SR Algorithm

3.4.1 Artifacts Due to Hue Channel

Color artifacts are occurred due to the angular dimension of the hue channel. Bilinear and bicubic interpolation methods and all of SR algorithms (DA, MAP, POCS and IBP) are applied to H, S and V channels respectively. In the experiments, all of three channels are handled with the same method. In Figure 13 and Figure 14, resultant images are shown. Also, gray scale view of the hue channel is shown in Figure 13-b. It is obviously recognized that, artifacts take place black and white transition parts of the gray scale representation of hue channel. Standard interpolation and SR methods are not suitable for hue channel because of its angular structure. These methods are successful in Cartesian coordinate color domains, like RGB.

Low resolution images are constructed by blurring, moving and down sampling the original image. These low resolution images are transferred to HSV color domain and each of LR images is divided into H, S, V channels. Standard interpolation methods and SR algorithms are applied to these three channels. Algorithm flowing chart is shown in Figure 12.

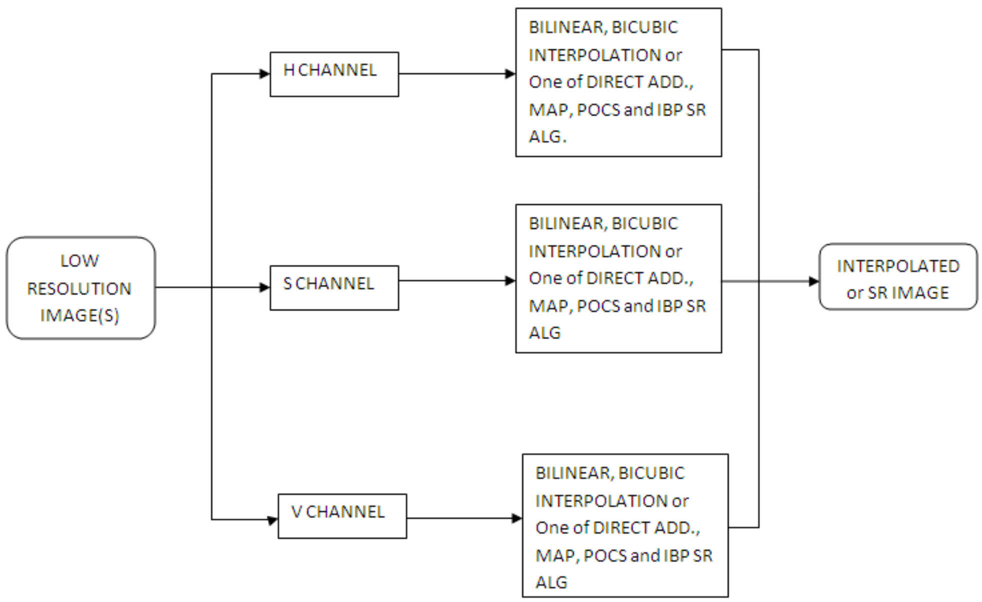

Figure 12. Algorithm Flowing Chart

a) b) c) d)

Figure 13. a) 512x512 Original Lena Image b) Gray Scale Projection of Hue Channel c) Bicubic Interpolation-3 channels d) Linear Interpolation-3 channels

a) b) c) d)

Figure 14. a) DA-3 channels (H, S, V) b) MAP-3 channels (H, S, V) c) POCS-3 channels (H, S, V) d) IBP-3 channels (H, S, V)

3.4.2 Proposed Method for Abolishing Color Artifacts

This thesis proposes three solution methods to get rid of the color artifacts on the super resolution image in HSV color domain. These methods are covered here in detail.

3.4.2.1 HSV1 - Applying Interpolation Method to Hue Channel and SR Algorithm to Value and Saturation Channels

The first suggested solution method is applying the nearest neighbor interpolation to the hue channel and SR algorithm to both value and saturation channels. First step is constructing low resolution images by blurring, moving and down sampling the original image. These low resolution images are transferred to HSV color domain and each of LR images is divided into H, S, V channels. All SR algorithms (DA, MAP, POCS, IBP) used in this thesis are applied to S and V channels respectively. Hue channel is processed by the simplest interpolation method. The nearest neighbor interpolation method is preferred to reduce the hue channel affect on SR reconstruction. Hence, S and V channels are luminance components of the image, their resolution enhancement is critical for SR scenario. Algorithm flowing chart is shown in Figure 15.

HSV1 Method (The first solution method) is useful for real time HSV domain video applications when high PSNR values are not needed. This solution method brings less computational complexity than applying SR algorithms to H, S, V channels.

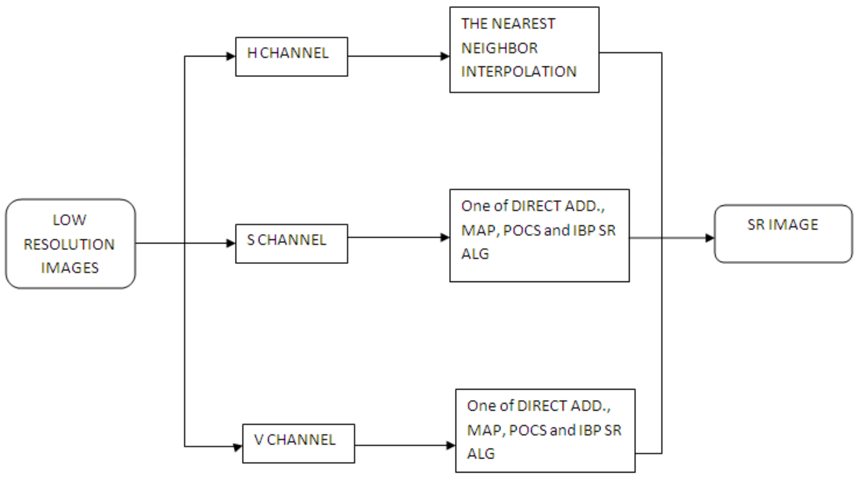

Figure 15. HSV1 Algorithm Flowing Chart

a) b) c)

Figure 16. a) LR Image b) Noisy LR Image c) 512x512 Original Lena Image

Figure 17. a) DA-HSV1 b) MAP-HSV1 c) POCS-HSV1 d) IBP-HSV1

3.4.2.2 HSV2 - Applying Interpolation and SR Algorithm to Hue Channel with Mask

If one need high PSNR values for HSV domain SR applications, SR algorithms can be applied to hue channel partially, as well. The second solution method (HSV2) suggests abolishing the color artifacts on SR image and getting higher PSNR values.

First step is the same as previous cases. That is constructing low resolution images by blurring, moving and down sampling the original image. These low resolution images are transferred to HSV color domain and each of LR images is divided into H, S, V channels. After, gray scale representation is obtained of hue channel (Figure 18-a.). As told before, black and white transition parts cause color artifacts. A mask is applied to hue channel to prevent the occurrence of these artifacts. This mask is used to cover the transition parts in Figure 18-a. The nearest neighbor interpolation method is applied to the masked part and one of SR algorithm is applied the remainder part of hue channel. HSV2 Algorithm following chart is given in Figure 19. Hue channel part of HSV2 algorithm steps are given below:

- A High pass filter is applied to the hue channel.
- Binary image is constructed with a threshold value after filtering the hue channel. Binary image is shown in Figure 18-b.
- Binary image is masked by dilating process to ignore the pixel errors. Mask is shown in Figure 18-c.
- Super resolved image is constructed by applying one of super resolution methods (DA, MAP, POCS, IBP) to hue channel.
- At the same time, the nearest neighbor interpolation method is applied to the hue channel to get super resolution image.
- With [*SR_Alg_hue* x (1 - *mask*) + *nni_hue* x *mask*] operation, HSV2 solution is obtained for hue channel.

a) b) c)

Figure 18. a) Gray Scale Projection of Hue Channel b) Threshold Binary Projection of Hue Channel after filtered with high pass filter c) Mask that is used for Hue Channel

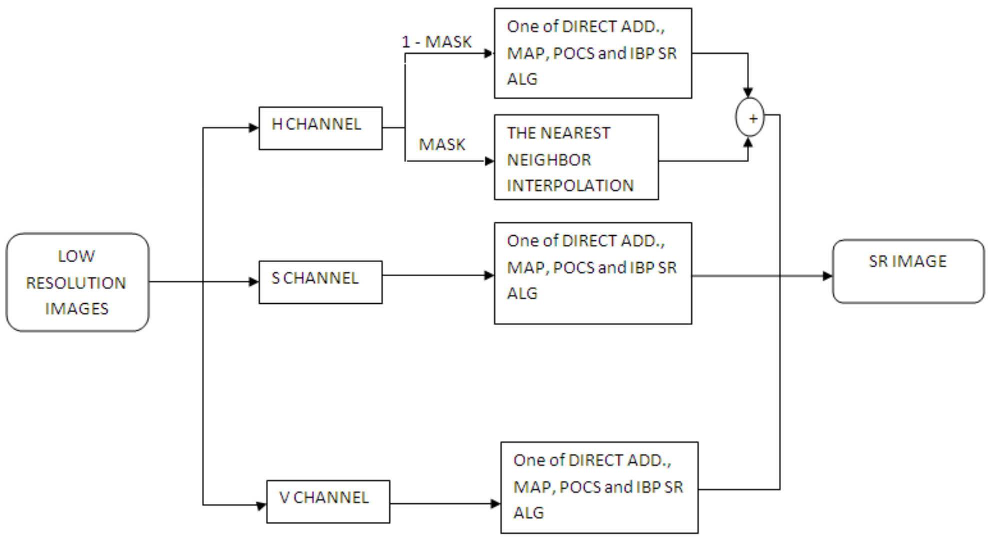

Figure 19. HSV2 Algorithm Flowing Chart

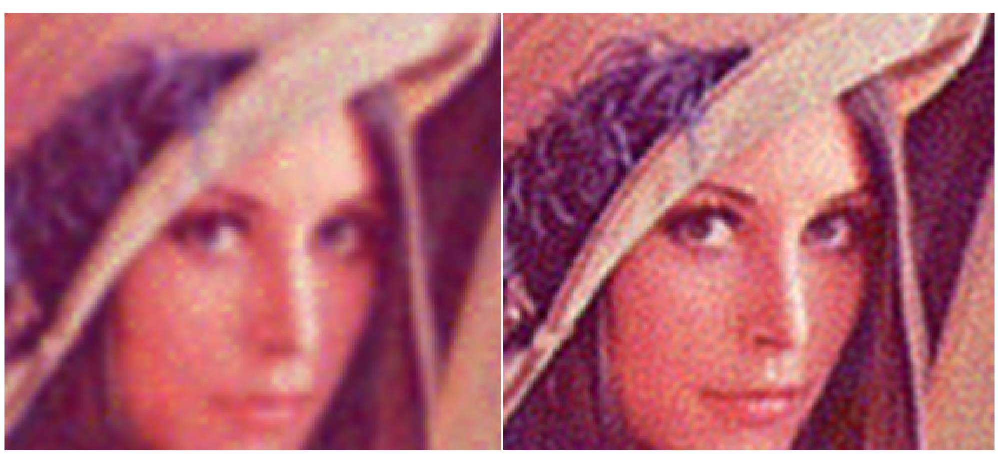

a) b)

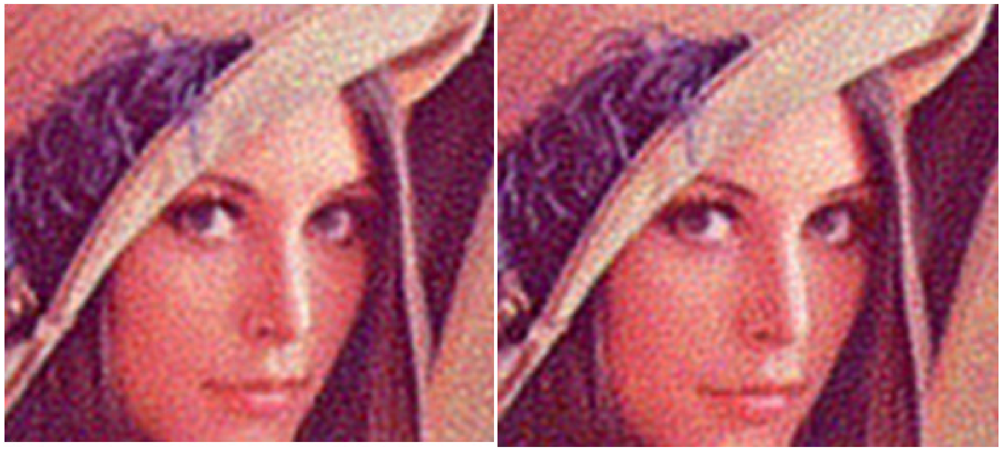

c) d)

Figure 20. a) DA – HSV2 b) MAP – HSV2 c) POCS – HSV3 d) IBP – HSV3

3.4.2.3 HSV3 - Applying SR Algorithm to Only Value Channel

The third solution method (HSV3) is applying super resolution algorithm to only value channel of HSV color domain. The nearest neighbor interpolation method is applied to the both hue and saturation channels. *Irani et al.* were applied super resolution algorithm to only Y channel of YIQ domain in their studies [7]. Because Y channel is the luminance component of the image in YIQ color domain. Predominantly, energy of the image is in brightness channels of the image and human visual system is more sensible to the changes of the luminance component. Because of these reasons, they follow the method that applying super resolution algorithm only to the luma component of the image which is Y channel. By the same point of view, HSV3 algorithm suggests to apply SR algorithm only to the value channel which contains the brightness data of the image in HSV color space. This experiment proves the importance of V channel of HSV color domain in SR reconstruction problem.

Low resolution images are constructed by blurring, moving and down sampling the original image. These low resolution images are transferred to HSV color domain and each of LR images is divided into H, S, V channels. All SR algorithms (DA, MAP, POCS, IBP) used in this thesis are applied to V channel respectively. Hue channel is processed by the simplest interpolation method which is the nearest neighbor interpolation. HSV3 algorithm flowing chart is given in Figure 21. The final SR image of each algorithm is given in Figure 22.

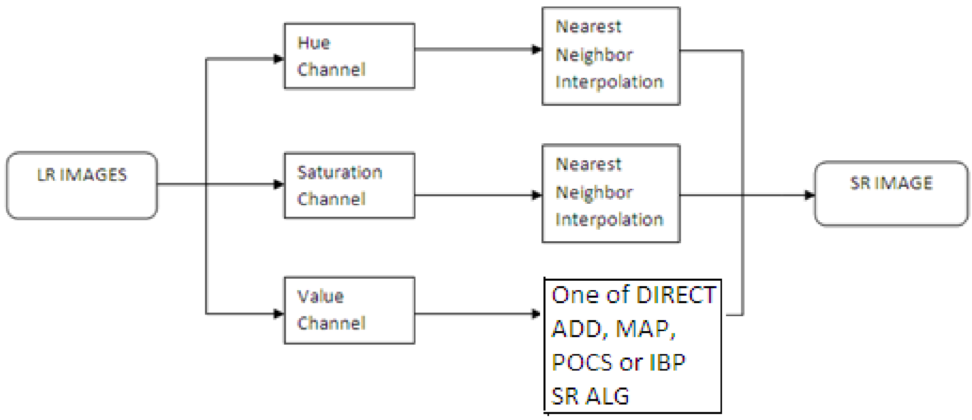

Figure 21. HSV3 Algorithm Flowing Chart

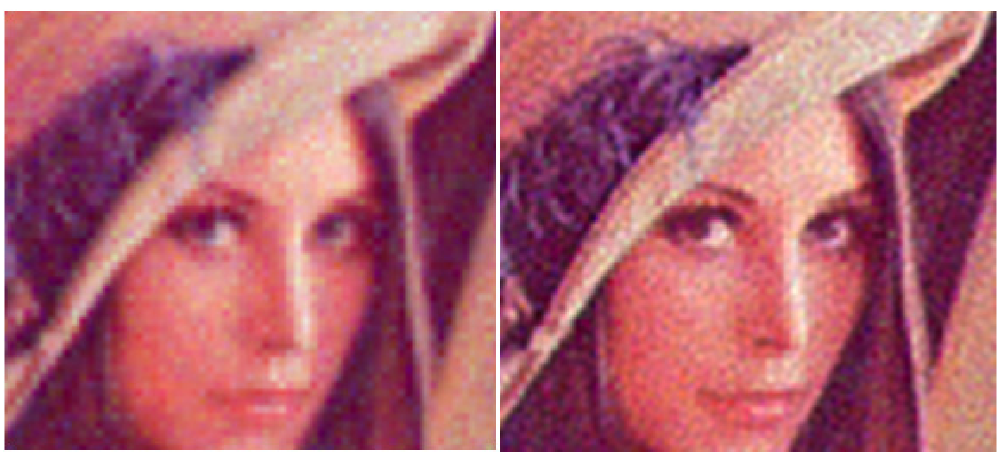

a) b)

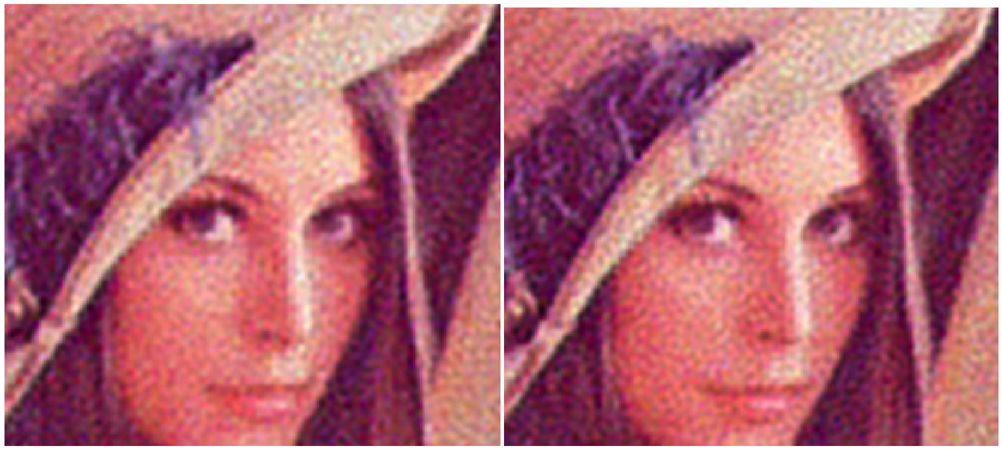

c) d)

Figure 22. a) DA – HSV3 b) MAP – HSV3 c) POCS – HSV3 d) IBP – HSV3

3.5 Color Super Resolution in YIQ Color Domain

3.5.1 Applying SR Algorithm to only Y Channel in YIQ Color Domain

In this thesis, YIQ color domain is the third color space studied on. SR algorithms and interpolation methods that are told before applied to YIQ color domain images. In YIQ color domain luminance and chrominance color components are obviously divided into two parts. Because of this reason, YIQ color domain is preferred to study on as the third color space. Y component carries the brightness data of the image and I and Q components carry the color data of the image. As told before details in the luminance component are important during reconstruction process. So, *Irani et al.* applied iterative back projection algorithm to Y cannel and non – uniform interpolation method to both I and Q channels [7]. By the same point of view, Y channel is processed with the SR algorithms and simple interpolation method is applied to I and Q channels, in our experiments.

Low resolution images are constructed by blurring, moving and down sampling the original image. These low resolution images are transferred to YIQ color domain and each of LR images is divided into Y, I, Q channels. All SR algorithms (DA, MAP, POCS, IBP) used in this thesis are applied to Y channel respectively. I and Q channels are processed by the simplest interpolation method which is the nearest neighbor interpolation. YIQ domain algorithm flowing chart is given in Figure 23. The final SR image of each algorithm is given in Figure 24.

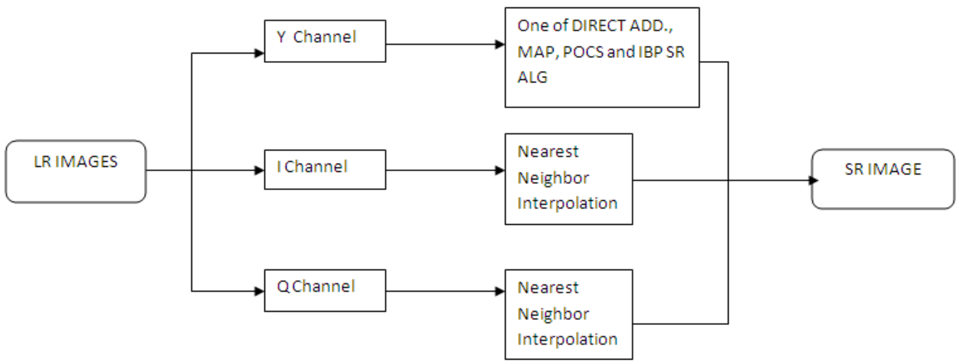

Figure 23. YIQ Domain Algorithm Flowing Chart

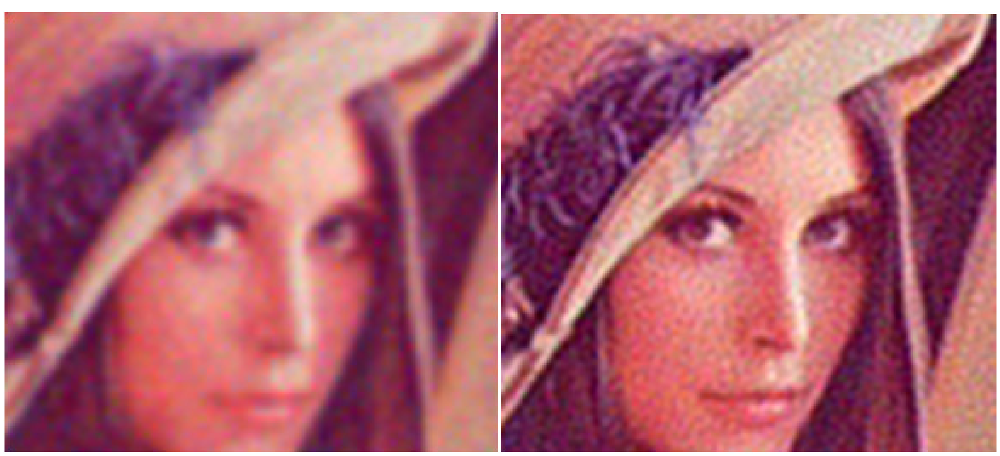

a) b)

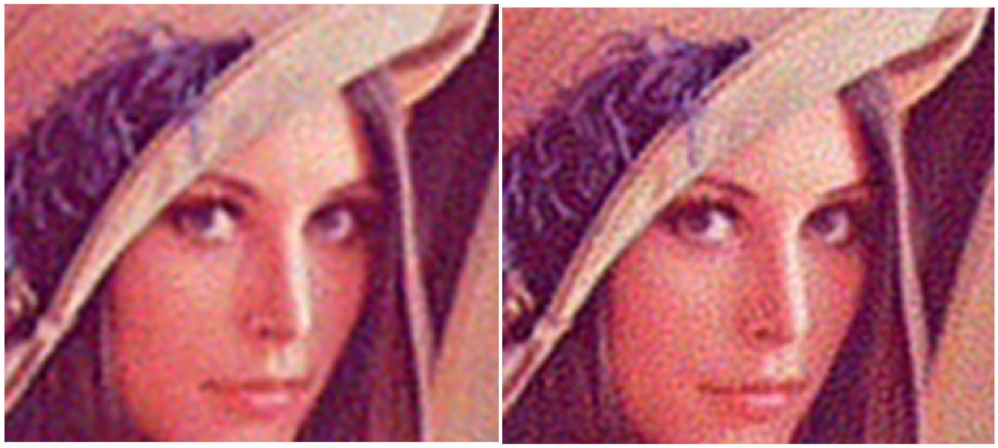

c) d)

Figure 24. a) DA - YIQ b) MAP - YIQ c) POCS - YIQ d) IBP – YIQ

CHAPTER 4

IMPLEMANTATION AND RESULTS

4.1 Experiments

Experiments start by constructing low resolution images from the original image. As an example, for 'Lena experiments' original image is 512X512 'Lena' image. Low resolution images are obtained according to the observation model in Figure 1. Original image is moved, blurred and down sampled to form eight number of low resolution images. Three channels of the original image are treated individually. First of all, each channel of the image is moved in the two pixels interval by small step sizes. Image movement is in both horizontal and vertical direction. These step sizes are changing between ± 2 pixels interval, randomly. Pixel shifts can be any number such as 0.5 pixels, 1 pixel or - 1.25 pixels... After moving step, image is blurred by 2X2 moving average filter. Image is convolved by the kernel shown in Equation 32.

$$Kernel = \frac{1}{4} \times \begin{bmatrix} 1/4 & 1/2 & 1/4 \\ 1/2 & 1 & 1/2 \\ 1/4 & 1/2 & 1/4 \end{bmatrix} \qquad (32)$$

After blurring, each monochrome image is down sampled by the decimation factor 2. Lastly, white, zero mean Gaussian noise is added on the images. Additive noise has standard deviation of 2 (256 scale). All super resolution algorithms given in this study are iterative, except Direct Addition. Iteration number is fix and sixteen for each experiment. Measurement of PSNR values versus algorithm iteration number show that sixteen is the optimum iteration number.

In the first five experiments, super resolution algorithms and proposed solution methods are applied different images. These images are widely used in the color SR reconstruction experiments. These five images are preferred for experiments because each one has different image features. 'Barbara' Image (exp. 1), is a textured image, 'peppers' Image (exp. 2) has bright colors, 'i-phone' Image (exp. 3) has a writing on it, 'airplane' Image (exp. 4) has smooth colors and 'zebra' Image has high frequency components.

Result images are given in seven image sets. In the first set, LR image, noisy LR image, original image and bicubic interpolation applied image in HSV color domain are demonstrated. Original image is starting point of the experiments. LR image is obtained after moving, blurring and down sampling the original image. Noisy LR image is formed after addition of Gaussian noise. Noisy LR image is enlarged by 2 with bicubic interpolation method in HSV domain. The second image set shows the result of four SR algorithms that are applied to three channels of RGB color domain image. The third, fourth, fifth and sixth image sets give the results of HSV color domain applications. In the third image set, SR algorithms are applied to three channels of HSV color domain image. Color artifacts are easily recognized on this set. In the fourth image set, SR algorithms are applied to S and V channels and the nearest neighbor interpolation method is applied to H channel of HSV color domain image. In other words, this image set shows the results of the first solution algorithm named HSV1 in Table 1. The fifth image set shows the results of the second solution method named HSV2 in Table 1. HSV2 suggests applying both SR algorithms and the nearest neighbor interpolation method to H channel with mask. The sixth image set shows the results of the third solution method named HSV3 in Table 1. In HSV3 method, only V channel is processed by SR algorithm and H and S channels are just interpolated. The last image set represents the results of YIQ color domain applications. SR algorithms are applied to only Y channel and I and Q channels are just interpolated with the nearest neighbor method.

In the last experiment, performance of algorithms is measured with respect to the changing parameters. Iteration number and noise standard deviation are changed and PSNR values of SR algorithms are measured. Results are given in tables and graphics. Also, computational complexity of algorithms is measured for proposed solution methods. Computational complexity measurements are done by time constraint. How long each algorithm takes is given in Table 8 and Table 9.

In this thesis, all PSNR values are compared in RGB color domain. The PSNR values that are given for HSV and YIQ color domains are obtained after converting the images to the RGB color domain because it is not sensible to compare the images in different color domains. Original input images are in RGB color domain and the output super resolution images are also shown in RGB color domain for demonstration.

4.1.1 Experiment 1

'Barbara' Image is texture based image. The aim of using this image is compare the SR algorithms' performance of reconstructing the details in the image. PSNR values of the SR algorithms for different color domains are given in Table 2.

a) b) c) d)

Figure 25. a) LR Image b) Noisy LR Image c) Original Image d) Bicubic-HSV

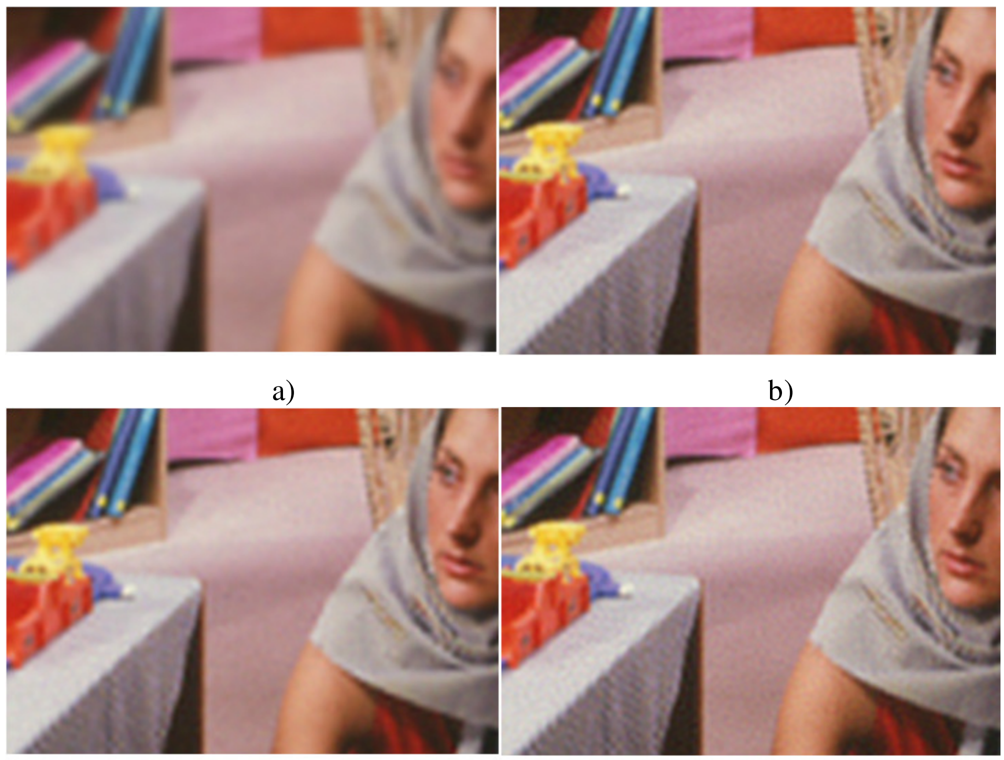

a) b)

c) d)

Figure 26. a) Direct Addition-RGB b) MAP-RGB c) POCS-RGB d) IBP-RGB

a) b)

c) d)

Figure 27. a) Direct Addition-HSV b) MAP-HSV c) POCS-HSV d) IBP-HSV

a) b)

c) d)

Figure 28. a) Direct Addition-HSV1 b) MAP-HSV1 c) POCS-HSV1 d) IBP-HSV1

a) b)

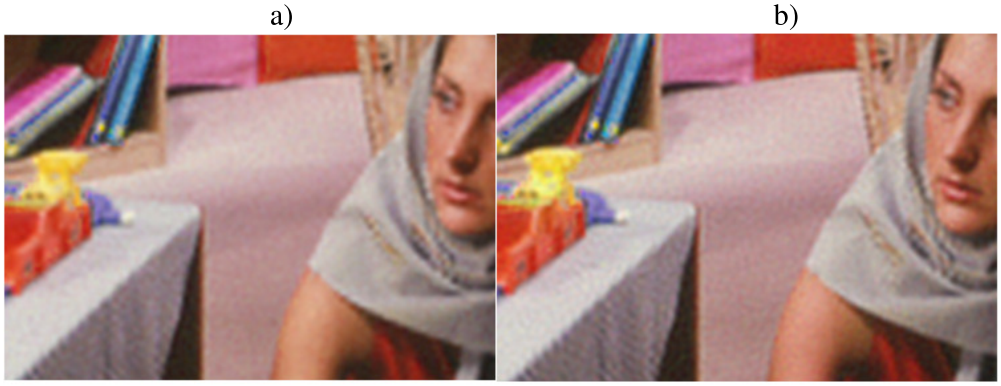

c) d)

Figure 29. a) Direct Addition-HSV2 b) MAP-HSV2 c) POCS-HSV2 d) IBP-HSV2

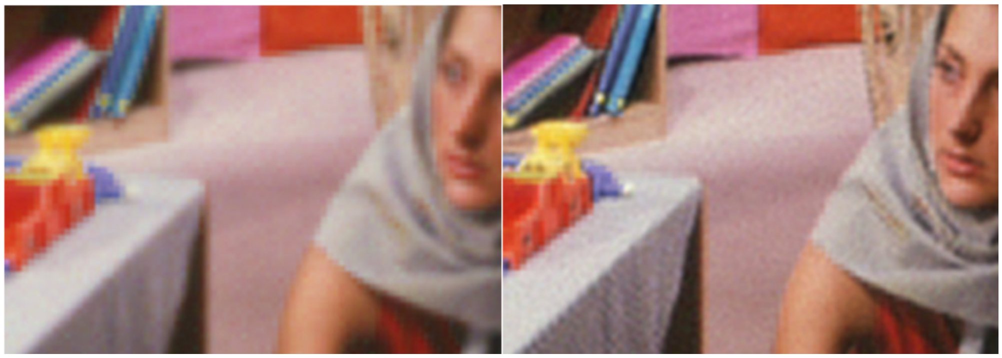

a) b)

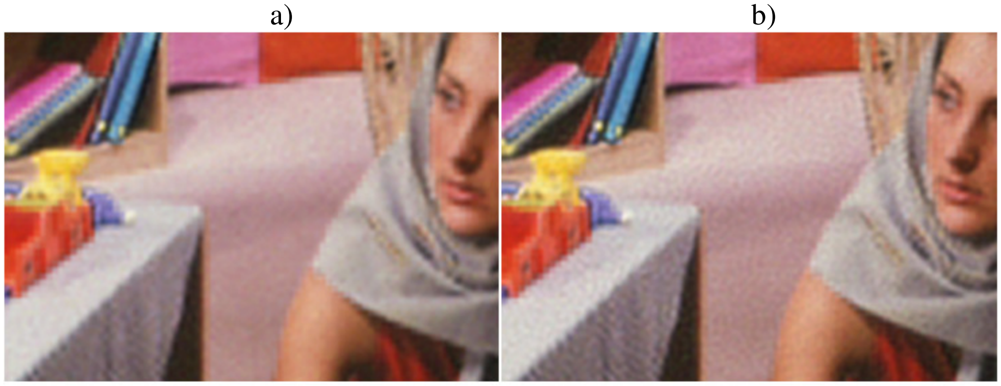

c) d)

Figure 30. a) Direct Addition-HSV3 b) MAP-HSV3 c) POCS-HSV3 d) IBP-HSV3

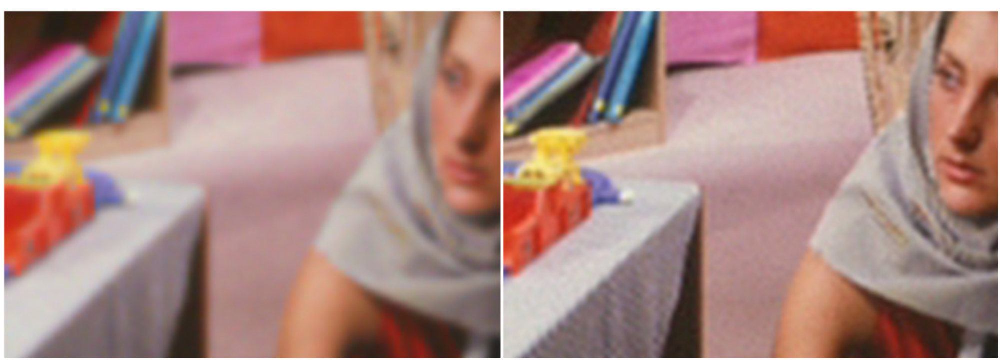

a) b)

c) d)

Figure 31. a) Direct Addition- YIQ b) MAP- YIQ c) POCS- YIQ d) IBP-YIQ

Table 2. PSNR Values for Experiment 1

	PSNR Values(dB)			
Color Domain	DA	MAP	POCS	IBP
RGB	23.26	27.47	27.09	27.51
HSV	22.21	25.96	25.64	26.05
HSV1	23.22	27.43	27.03	27.48
HSV2	23.24	27.41	27.05	27.46
HSV3	23.50	26.85	26.53	26.93
YIQ	23.33	27.20	26.70	27.28

4.1.2 Experiment 2

'Peppers' Image has bright colors. The aim of using this image is compare the SR algorithms' performance at color transition parts of the image. These kinds of data images are good to recognize the artifacts due to color bands correlations. PSNR values of the SR algorithms for different color domains are given in Table 3.

a) b) c) d)

Figure 32. a) LR Image b) Noisy LR Image c) Original Image d) Bicubic-HSV

a) b) c) d)

Figure 33. a) Direct Addition-RGB b) MAP-RGB c) POCS-RGB d) IBP-RGB

a) b) c) d)

Figure 34. a) Direct Addition-HSV b) MAP-HSV c) POCS-HSV d) IBP-HSV

a) b) c) d)

Figure 35. a) Direct Addition-HSV1 b) MAP-HSV1 c) POCS-HSV1 d) IBP-HSV1

a) b) c) d)

Figure 36. a) Direct Addition-HSV2 b) MAP-HSV2 c) POCS-HSV2 d) IBP-HSV2

a) b) c) d)

Figure 37. a) Direct Addition-HSV3 b) MAP-HSV3 c) POCS-HSV3 d) IBP-HSV3

a) b) c) d)

Figure 38. a) Direct Addition-YIQ b) MAP-YIQ c) POCS-YIQ d) IBP-YIQ

Table 3. PSNR Values for Experiment 2

	PSNR Values(dB)			
Color Domain	DA	MAP	POCS	IBP
RGB	24.13	33.05	30.45	32.93
HSV	21.18	26.45	25.21	26.30
HSV1	24.64	30.52	29.47	30.33
HSV2	24.47	30.44	30.05	30.08
HSV3	25.07	29.06	28.43	29.00
YIQ	24.48	27.86	28.95	30.39

4.1.3 Experiment 3

'i-phone' Image has writing on it. The aim of using this image is compare the SR algorithms' performance of reconstructing the writings on the images. This experiment is good for recognizing the difference between the SR algorithms visually. PSNR values of the SR algorithms for different color domains are given in Table 4.

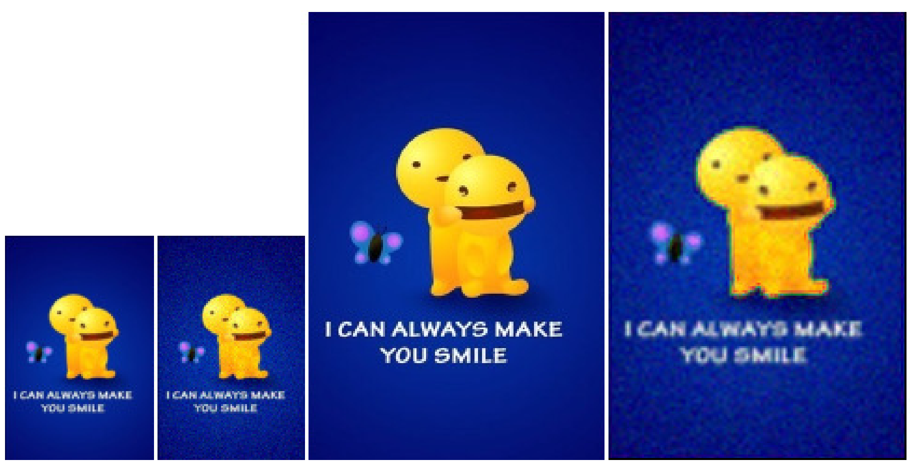

a) b) c) d)

Figure 39. a) LR Image b) Noisy LR Image c) Original Image d) Bicubic-HSV

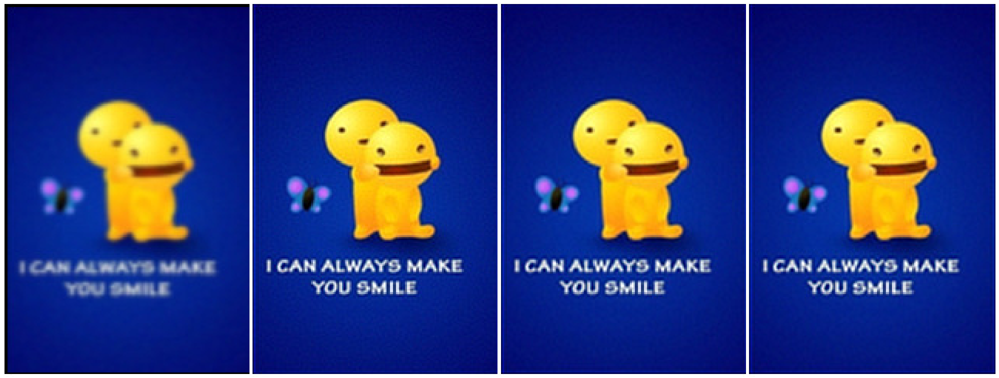

a) b) c) d)

Figure 40. a) Direct Addition-RGB b) MAP-RGB c) POCS-RGB d) IBP-RGB

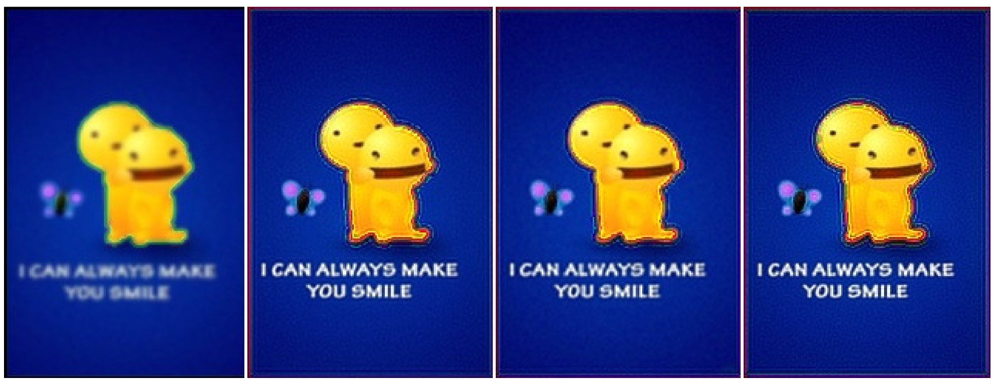

a) b) c) d)

Figure 41. a) Direct Addition-HSV b) MAP-HSV c) POCS-HSV d) IBP-HSV

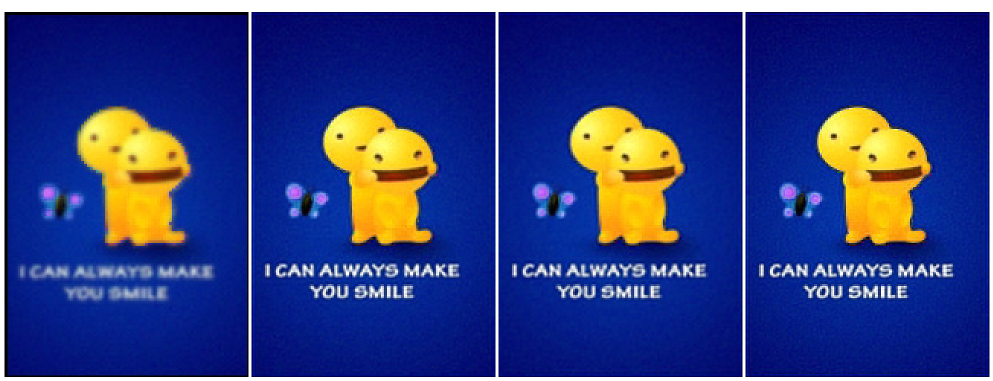

a) b) c) d)

Figure 42. a) Direct Addition-HSV1 b) MAP-HSV1 c) POCS-HSV1 d) IBP-HSV1

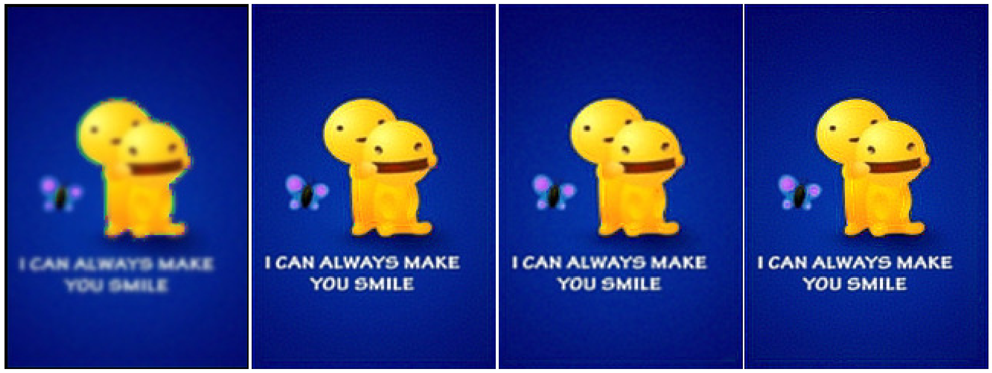

a) b) c) d)

Figure 43. a) Direct Addition-HSV2 b) MAP-HSV2 c) POCS-HSV2 d) IBP-HSV2

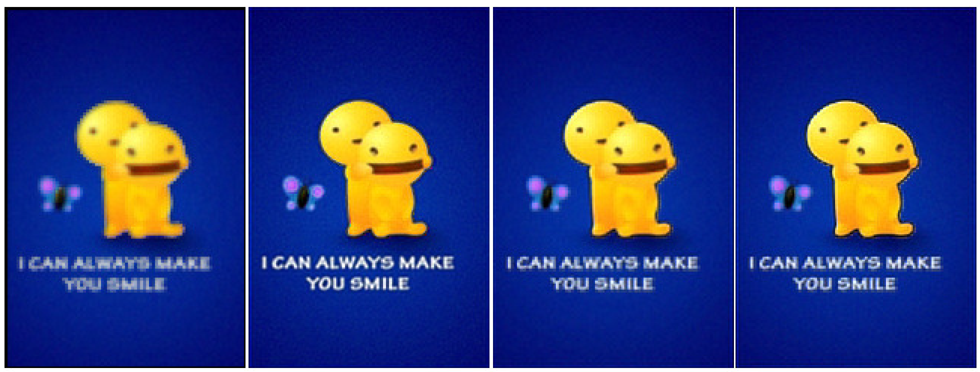

a) b) c) d)

Figure 44. a) Direct Addition-HSV3 b) MAP-HSV3 c) POCS-HSV3 d) IBP-HSV3

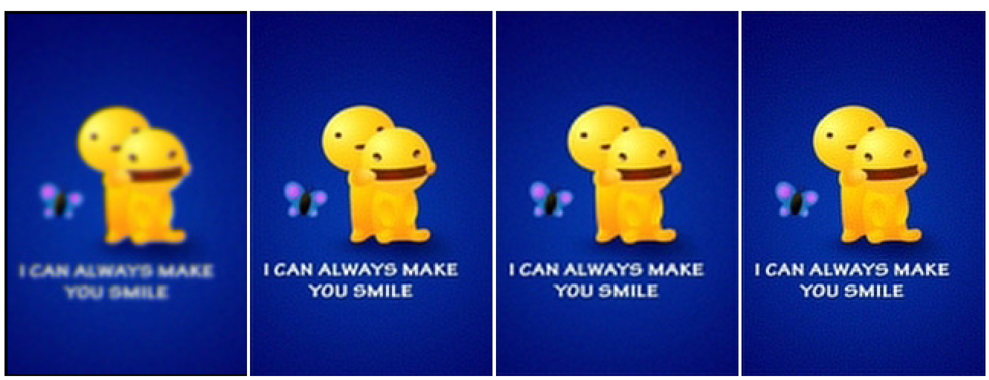

a) b) c) d)

Figure 45. a) Direct Addition-YIQ b) MAP-YIQ c) POCS-YIQ d) IBP-YIQ

Table 4. PSNR Values for Experiment 3

	PSNR Values(dB)			
Color Domain	DA	MAP	POCS	IBP
RGB	16.35	25.34	24.12	26.86
HSV	16.06	19.60	20.01	19.42
HSV1	16.44	24.29	23.14	24.93
HSV2	16.23	24.34	23.16	24.91
HSV3	17.20	22.27	21.53	22.80
YIQ	16.19	22.51	21.77	23.39

4.1.4 Experiment 4

'Airplane' Image has smooth colors. The aim of using this image is compare the SR algorithms' performance on smooth colors. PSNR values of the SR algorithms for different color domains are given in Table 5.

a) b) c) d)

Figure 46. a) LR Image b) Noisy LR Image c) Original Image d) Bicubic-HSV

a) b) c) d)

Figure 47. a) Direct Addition-RGB b) MAP-RGB c) POCS-RGB d) IBP-RGB

a) b) c) d)

Figure 48. a) Direct Addition-HSV b) MAP- HSV c) POCS- HSV d) IBP- HSV

a) b) c) d)

Figure 49. a) Direct Addition-HSV1 b) MAP- HSV1 c) POCS- HSV1 d) IBP- HSV1

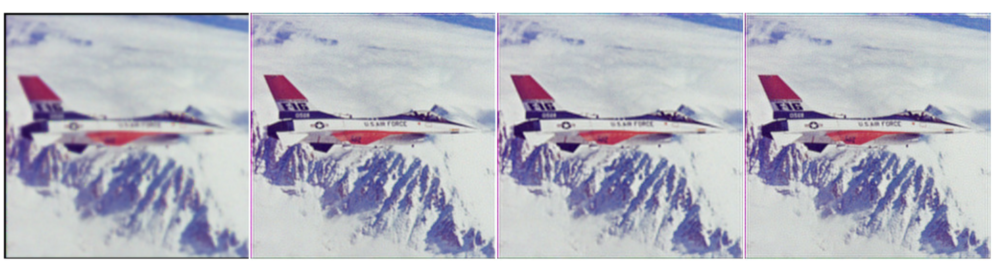

a) b) c) d)

Figure 50. a) Direct Addition-HSV2 b) MAP- HSV2 c) POCS- HSV2 d) IBP- HSV2

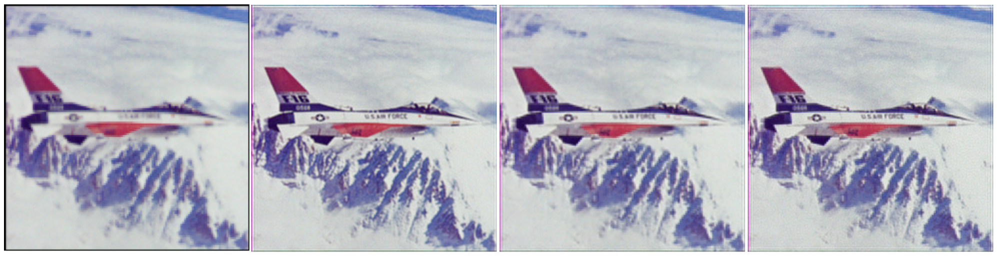

a) b) c) d)

Figure 51. a) Direct Addition-HSV3 b) MAP- HSV3 c) POCS- HSV3 d) IBP- HSV3

a) b) c) d)

Figure 52. a) Direct Addition-YIQ b) MAP-YIQ c) POCS-YIQ d) IBP-YIQ

Table 5. PSNR Values for Experiment 4

	PSNR Values(dB)			
Color Domain	DA	MAP	POCS	IBP
RGB	19.19	29.98	28.39	30.47
HSV	18.87	28.34	27.09	27.44
HSV1	19.34	28.95	27.36	28.92
HSV2	19.24	29.00	27.44	28.98
HSV3	20.42	24.95	24.32	25.03
YIQ	19.06	27.83	26.65	27.90

4.1.5 Experiment 5

'Zebra' Image has high frequency components. The aim of using this image is compare the SR algorithms' performance at the black and white transition parts of the image. PSNR values of the SR algorithms for different color domains are given in Table 6.

a) b) c) d)

Figure 53. a) LR Image b) Noisy LR Image c) Original Image d) Bicubic-HSV

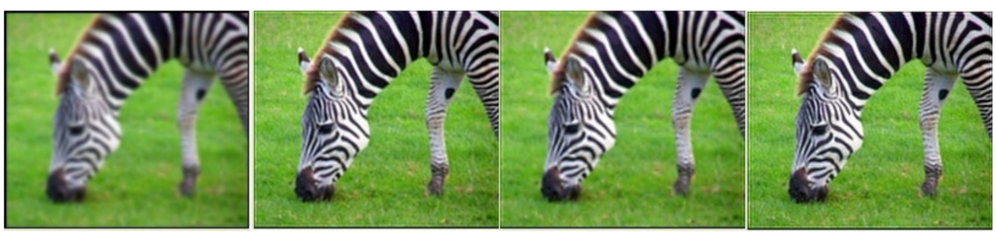

a) b) c) d)

Figure 54. a) Direct Addition-RGB b) MAP-RGB c) POCS-RGB d) IBP-RGB

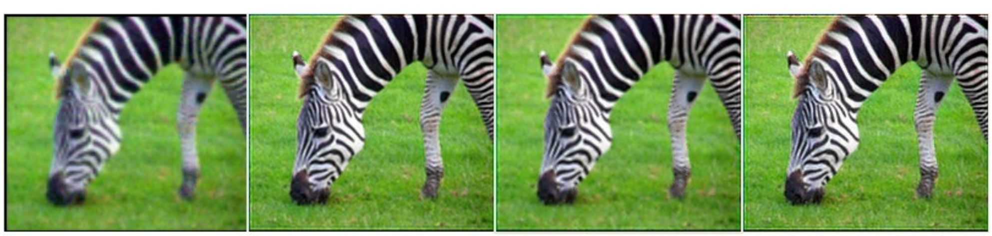

a) b) c) d)

Figure 55. a) Direct Addition-HSV b) MAP-HSV c) POCS-HSV d) IBP-HSV

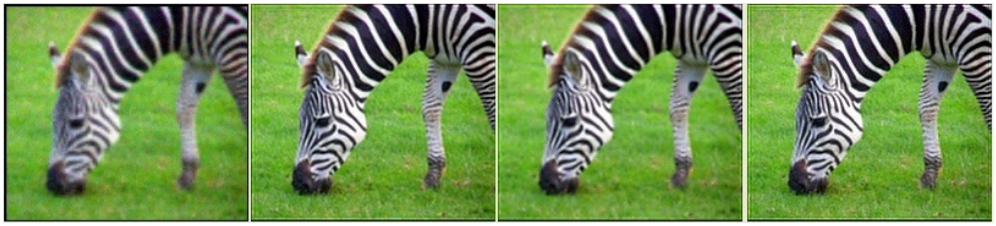

a) b) c) d)

Figure 56. a) Direct Addition-HSV1 b) MAP-HSV1 c) POCS-HSV1 d) IBP-HSV1

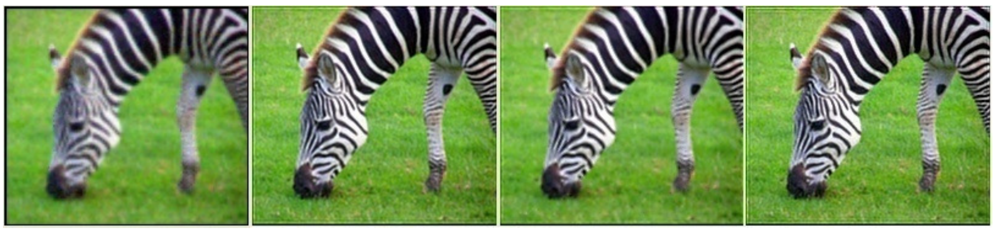

a) b) c) d)

Figure 57. a) Direct Addition-HSV2 b) MAP-HSV2 c) POCS-HSV2 d) IBP-HSV2

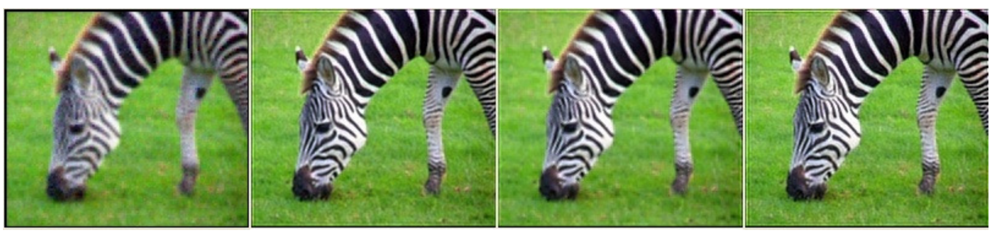

a) b) c) d)

Figure 58. a) Direct Addition-HSV3 b) MAP-HSV3 c) POCS-HSV3 d) IBP-HSV3

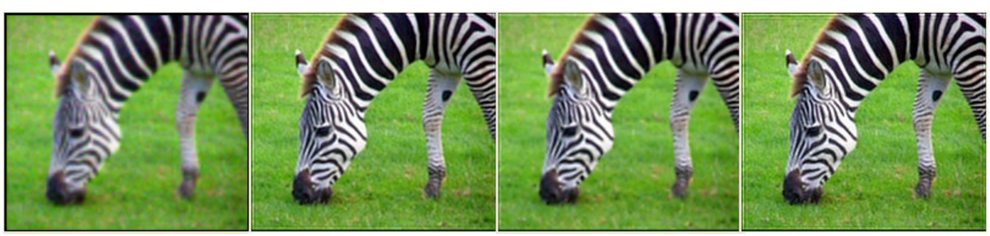

a) b) c) d)

Figure 59. a) Direct Addition-YIQ b) MAP- YIQ c) POCS- YIQ d) IBP- YIQ

Table 6. PSNR Values for Experiment 5

	PSNR Values(dB)			
Color Domain	DA	MAP	POCS	IBP
RGB	24.79	30.30	27.69	30.58
HSV	23.76	29.60	27.72	29.07
HSV1	23.28	29.88	27.82	30.31
HSV2	23.70	30.05	27.91	30.32
HSV3	23.59	27.90	26.72	28.22
YIQ	25.60	28.96	27.06	29.47

4.1.6 Experiment 6

In the last experiment, parameters' effects on SR algorithms are investigated. In Figure 60, changing PSNR values of MAP, POCS and IBP SR algorithms are given versus different number of iterations. These graphics prove that, sixteen is the optimum iteration number. It is obviously clear that after sixteen, variations of PSNR values are small.

Noise standard deviation is another parameter that affects the performance of the algorithms. Increasing the amount of noise standard deviation causes to decrease of PSNR values. It is an expected result. Figure 61is more important that it compares the performance of SR algorithms with respect to each other, in noisy cases.

Computational load analysis is one of the performance measurement methods for SR algorithms. Two different images are used in this experiment. Image sizes are 256X256 and 512X512. Process time of each SR algorithms for RGB and HSV color domains is given in Table 8 and Table 9. First, SR algorithms are applied to three channels of the images in RGB and HSV color domains and time measurements are shown in Table 8. Secondly, three suggested solution methods are applied to the images and time measurements are shown in Table 9. Comparison of Table 8 and Table 9 proves decreasing of computational complexity.

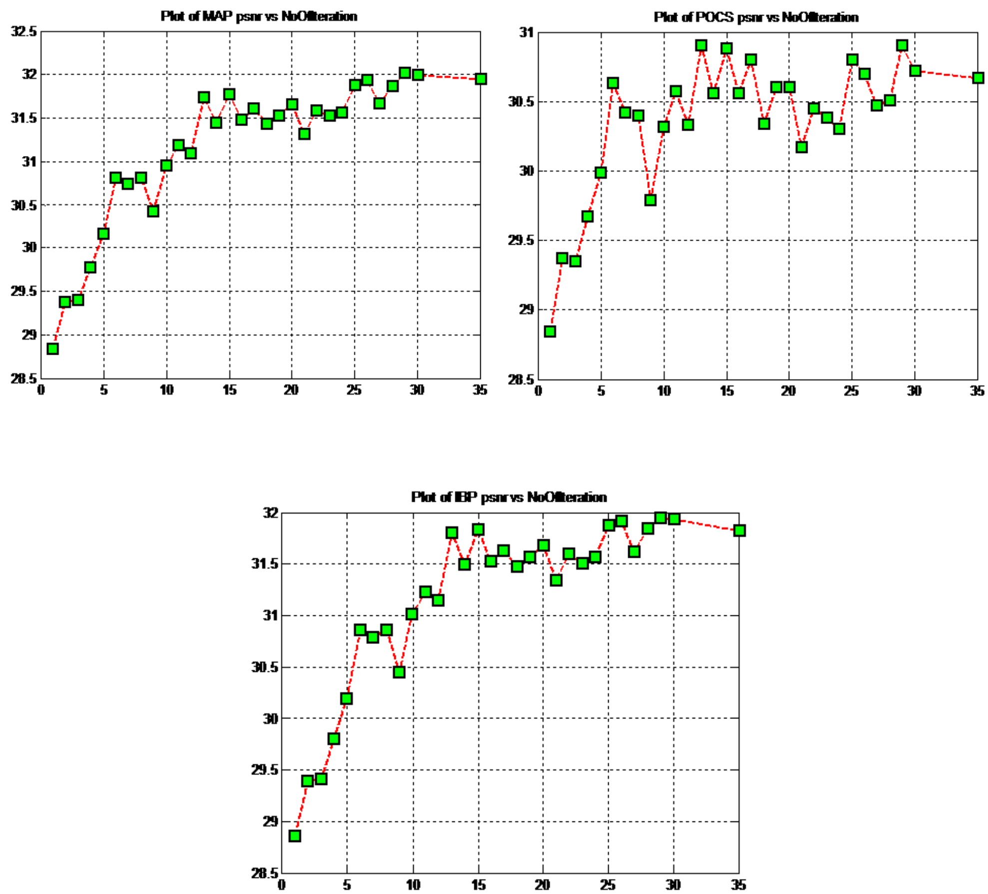

Figure 60. No Of Iteration vs MAP, POCS and IBP algorithms PSNR values

Table 7. PSNR Values for different values of Noise Standard Deviation

Noise Standard Deviation	PSNR Values (dB)			
	MAP	POCS	IBP	DA
2	31.46	30.04	31.52	21.56
4	30.02	29.53	29.99	21.48
6	28.68	29.03	28.58	21.40
8	27.15	28.08	26.98	21.32
10	25.95	27.06	25.76	21.30

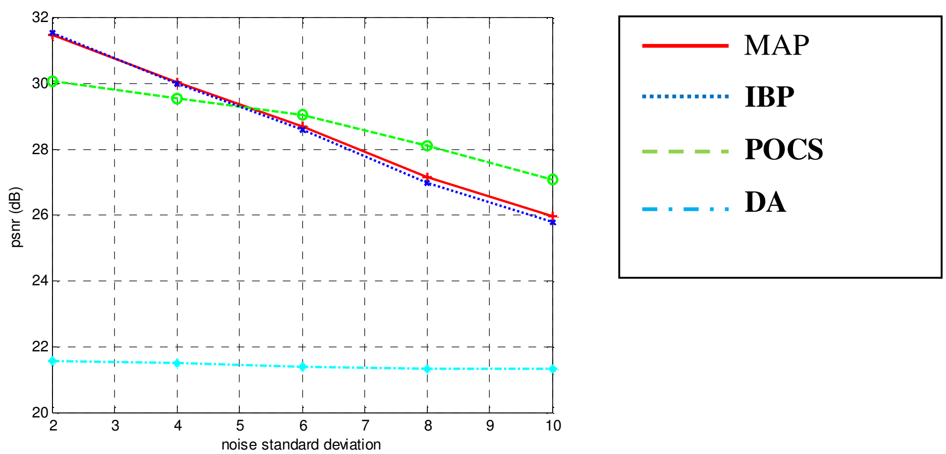

Figure 61. PSNR Values for MAP, POCS, IBP, DA Algorithms vs Noise Standard Deviation

Table 8. Time Measurements

	RGB Experiments		HSV1 Experiments	
SR ALG.	256X256 Image	512X512 Image	256X256 Image	512X512 Image
DA	0.88 s	2.10 s	0.89 s	2.19 s
MAP	5.57 s	19.52 s	10.93 s	39.29 s
POCS	5.60 s	19.63 s	11.00 s	38.52 s
IBP	5.07 s	17.52 s	9.79 s	34.87 s

Table 9. Time Measurements

	HSV1 Experiments		HSV2 Experiments		HSV3 Experiments	
SR ALG.	256X256 Image	512X512 Image	256X256 Image	512X512 Image	256X256 Image	512X512 Image
DA	0.74 s	1.54 s	1.85 s	3.18 s	0.42 s	0.99 s
MAP	3.72 s	13.20 s	6.33 s	20.66 s	3.27 s	12.87 s
POCS	3.81 s	12.99 s	6.56 s	20.42 s	3.85 s	13.98 s
IBP	3.42 s	11.86 s	5.96 s	18.78 s	3.05 s	11.98 s

4.2 RESULTS

Conducted experiments mainly aim to compare the performance of monochrome SR algorithms on color images. Each SR algorithm is applied to five different images on RGB color domain. If super resolution results are examined carefully, Direct Addition (DA) algorithm always gives blurred results because DA algorithm is not iterative based, it is the simplest SR algorithm based on shift and addition operations. It directly shifts and adds the low resolution images onto a common grid with a specified resolution factor. Outputs of MAP, POCS and IBP SR algorithms are almost similar to each other and these three algorithms have better performance than the former algorithm on color images. These three algorithms minimize their cost function iteratively. If these three algorithms are compared in detailed, POCS SR result is smoother than SR results of MAP and IBP algorithms because of the boundaries used in the POCS algorithm. Errors that are smaller than these boundaries don't contribute to the final result in POCS framework. POCS algorithm brings ringing effect on color images. These ringing effects become more distinct when the value of boundaries is increased in the algorithm. When PSNR values are compared, generally results of MAP and IBP algorithms are closer to each other and better than POCS algorithm's results. MAP and IBP algorithms minimize almost the same cost function, except the high frequency regularization term used in MAP algorithm. Due to this regularization term, MAP algorithm is better in noisy cases. As noise level is increased, MAP algorithm gives smoother and higher quality SR images than IBP algorithm.

In all experiments 1 through 5, color distortions occurred when SR algorithms are applied to three channels in HSV color domain and all of three solution methods solved this problem. Output SR images of HSV1 and HSV2 methods are better than the output of HSV3 method. If the images are analyzed carefully, HSV1 and HSV2 methods are successful in reconstructing the details at the edge of the figures as the sharper edges illustrate. Output SR image of HSV3 method has a little bit mosaic (zipper) effect at the edges. 'Zebra' image is a good example to demonstrate this argument. If zoomed into black and white transitions, difference can be recognized. PSNR results support the experimental results. PSNR values of HSV1 and HSV2 are close to each other and higher than the PSNR values of HSV3. YIQ color domain experiments are achieved to compare the results with the outputs of HSV3 solution method. In both methods, SR algorithms are applied on one color channel that is the luminance component. This idea works in YIQ color domain better than HSV color domain because just Value channel does not stand for only the luminance component of the image but also includes chroma information. Saturation channel also carries the brightness data, which implies that using two channels in SR reconstruction is better in HSV color domain.

Experiment 6 demonstrates that 16 is the optimum iteration number. After that number, performance of algorithms converges to a certain value. So, all iterative algorithms use 16 iterations for optimum performance and efficiency. This experiment also illustrates the effect of noise level on the algorithms. POCS algorithm is more stable than the other iterative algorithms because of the boundary constraint. MAP algorithm is better than IBP algorithm for suppressing the Gaussian noise because of the high frequency regularization term. Computational load analysis is given in experiment 6 as well. HSV1 and HSV3 solution methods reduce the computational complexity noticeably with respect to the three channels application of SR algorithms in both RGB and HSV domains. HSV2 solution method is used to mask the hue channel. So in this case, masking process brings extra computational load. This extra load is due to the least efficient software. But it still reduces the computation time as compared with three channel SR reconstruction in HSV color domain due to reduced data load.

In time measurement experiments of DA algorithm, process time of 216x216 image is almost half of the process time of 512x512 image. But it is expected to be one quarter of process time of bigger image. The kernel used for shifting and adding operations is a separable filter.

CHAPTER 5

CONCLUSIONS AND FUTURE WORK

5.1 CONCLUSIONS

As a conclusion, in this thesis basically three different super resolution algorithms are proposed for HSV color domain images and performance of monochrome SR algorithms on color images are tested in RGB, HSV and YIQ color domains.

The first solution method offers applying SR algorithms to the Saturation and Value channels and the simplest interpolation method to Hue channel of the HSV color domain images. This algorithm is useful for real time HSV domain video applications when computational performance of the process is critical. The second solution method suggests applying SR algorithm to hue channel partially. A mask is constructed to apply both interpolation and SR algorithm to hue channel. Masking process helps to ignore the pixel errors due to the color transition parts of the hue channel. This solution method is suitable for the applications where high PSNR values are needed. The third solution method considers only Value channel in SR reconstruction scenario because it is the luminance component of the image. *Irani et. al.* applied the same idea in YIQ color domain [7]. This method is more successful in YIQ color domain than HSV color domain. Hence, S also contains the brightness data of the image as well as the V channel. Because of this reason HSV1 method gives better results than HSV3 method.

In RGB color domain three channels (R, G, B) have equal importance in SR image reconstruction. All of three channels contain color and brightness data of the image together so SR algorithms are applied to three channels. In HSV color domain, S and V channels are useful for SR reconstruction. Just H channel carry pure color data and both of two remaining channels carry intensity information. Unlike the others, in YIQ color domain channels can be separated into luminance and chrominance channels. That Y is luminance channel; it is enough to use only this channel in SR reconstruction applications.

Iterative based SR algorithms are better than DA algorithm in color super resolution. SR result of DA algorithm is blurred in all color domains when compared the other SR methods. SR images of MAP and IBP algorithms are sharper than the output of POCS. MAP and IBP are good in reconstruction of the details and edges of the images. Also MAP algorithm exceeds IBP in noisy cases due to the regularization term in cost function. Also POCS algorithm is more stable and successful than MAP and IBP for noisy color images because of the boundary constraints.

5.2 FUTURE WORK

In recent color super resolution studies, applying demosaicking after super resolution algorithms is found wide acceptance to beat the color artifacts on the SR image. As a future work, a different color super resolution algorithm which is concerned with the demosaicking effect can be implemented and the results can be compared with the outputs of suggested solution methods in this thesis. POCS algorithm is more stable than the other SR algorithms against noise. Also, noise constraint can be added to POCS algorithm to get better results in noisy cases.

REFERENCES

[1] R. Y. Tsai and T. S. Huang, "Multiframe image restoration and registration," in Advances in Computer Vision and Image Processing, T. S. Huang, Ed. JAI Press, 1984, vol. 1, pp. 317 – 339.

[2] A. M. Tekalp, M. K. Ozkan, and M. I. Sezan, "High-esolution image reconstruction from lower-resolution image sequences and space varying image restoration," in Proc. IEEE Int. Conf. Acoustics, Speech and Signal Processing (ICASSP), San Francisco, CA., vol. 3, Mar. 1992, pp. 169-172.

[3] S. Borman and R. L. Stevenson, "Super-resolution from image sequences A review," in Proc. 1998 Midwest Symp. Circuits and Systems, 1999, pp. 374-378.

[4] S. C. Park, M. K. Park, and M. G. Kang, "Super-resolution image reconstruction: A technical review," IEEE Signal Processing Mag., vol. 20, pp. 21-36, May 2003.

[5] B. C. Tom and A. Katsaggelos, "Resolution Enhancement of Monochrome and Color Video Using Motion Compensation," IEEE Trans. Image Processing, Vol. 10, no. 2, pp. 278 – 287, Feb. 2001.

[6] N. R. Shah and A. Zakhor, “Resolution Enhancement of Color Video Sequences,” IEEE Trans. Image Processing, Vol. 8, no. 6, pp. 879 – 885, June 1999.

[7] M. Irani and S. Peleg, “Improving Resolution by Image Registration,” CVGIP: Graphical Models and Image Proc., Vol. 53, pp. 231 – 239, May 1991.

[8] S. Farsiu, M Elad and P. Milanfar, “Multi-Frame Demosaicing and super-Resolution of Color Images” IEEE Trans. Image Processing, Vol. 15, no. 1, pp. 141 – 159, Jan. 2006.

[9] R. H. Hibbard, “Apparatus and method for adaptively interpolating a full color image utilizing luminance gradients,” U.S. Patent 5,382,976, 1995.

[10] C. A. Laroche and M. A. Prescott, “Apparatus and method for adaptively interpolating a full color image utilizing chrominance gradients,” U.S. Patent 5,373,322, 1994.

[11] J. E. Adams and J. F. Hamilton, “Design of practical color filter array interpolation algorithms for digital cameras,” In Proc. SPIE, volume 3028, pages 117–125, 1997

[12] J. W. Glotzbach, R. W. Schafer and K. Illgner, “A Method of color filter array interpolation with alias cancellation properties,” In Proc. IEEE Int. Conf. Image Processing, volume 1, pages 141–144, 2001.

[13] B. K. Gunturk, Y. Altunbasak and R. M. Mersereau , “Color plane interpolation using alternating projections,” IEEE Trans. Image Processing, 11(9):997–1013, 2002.

[14] J. Mukherjee, R. Parthasarathi and S. Goyal, “Markov random field processing for color demosaicing,” Pattern Recognition Letters, 22(3-4):339–351, 2001.

[15] O. Kapah and H. Z. Hel-Or, “Demosaicing using artificial neural networks,” In Proc. SPIE, Vol. 3962, pp. 112–120, 2000.

[16] K. Hirakawa and T. W. Parks, “Adaptive homogeneity-directed demosaicing algorithm,” Proc. IEEE Int. Conf. Image Processing, 3:669–672, 2003.

[17] S. Süsstrunk, R. Buckley and S. Swen, ‘”Standard RGB color spaces”, In: 7th IS&T/SID Color Imaging Conference, Vol. 7, pp. 127 – 134, 1999.

[18] D. Keren, S. Peleg, and R. Brada, "Image sequence enhancement using subpixel displacements," in Proceedings of the IEEE Computer Society Conference on Computer Vision and Pattern Recognition, pp. 742 – 746, June 1988.

[19] K. Aizawa, T. Komatsu, and T. Saito, "Acquistion of very high resolution image using stereo cameras," in Visiul Communications and Image Processing, Vol. 1605 of Proceedings of the SPIE, pp. 318 – 328, 1991.

[20] R. Franke, "Smooth interpolation of scattered data by local thin plate splines," Computers and Mathematics with Applications, Vol. 8, no. 4, pp. 273 – 281, 1982.

[21] K. D. Sauer and J. P. Allebach, "Iterative reconstruction of band-limited images from nonuniformly spaced samples," IEEE Transactions on Circuits and Systems, Vol. 34, no. 12, pp. 1497 – 1506, 1987.

[22] S. Yeh and H. Strk "Iterative and one-step reconstruction from nonuniform samples by convex projections," Journal of the Optical Society of America A, Vol. 7, pp. 491 – 499, 1990.

[23] B. R. Frieden and H. G. Aumann, "Image reconstruction from multiple 1-D scans using filtered localized projection," Applied Optics, Vol. 26, no. 17, pp. 3615 – 3621, Sept. 1987.

[24] M. Irani and S. Peleg, "Super resolution from image sequences," in Proceedings of the 10th International Conference on Pattern Recognition, Atlantic City, NJ, Vol. 2, pp. 115 – 120, June 1990.

[25] M. Irani and S. Peleg, "Motion analysis for image enhancement: Resolution, occlusion and transparency," Journal of Visual Communications and Image Representation, vol. 4, pp. 324–335, Dec. 1993.

[26] M. Irani, B. Rousso, and S. Peleg, "Computing occluding and transparent motions," International Journal of Computer Vision, vol. 12, no. 1, pp. 5–16, Feb. 1994.

[27] R. R. Schultz and R. L. Stevenson, "Improved definition image expansion," in Proceedings of the IEEE International Conference on Acoustics, Speech and Signal Processing, San Francisco, CA, Mar. 1992, vol. 3, pp. 173–176.

[28] B. C. Tom and A. K. Katsaggelos, "Reconstruction of a high-resolution image by simultaneous registration, restoration and interpolation of low-resolution images," in Proceedings of the IEEE International Conference on Image Processing, Washington, DC, 1995, vol. 2,pp. 539–542.

[29] H. Stark and P. Oskoui, "High-resolution image recovery from image-plane arrays, using convex projections," Journal of the Optical Society of America A, vol. 6, no. 11, pp. 1715–1726, 1989.

[30] G. T. Herman, Image Reconstruction from Projections: The Fundamentals of Computerized Tomography, Academic Press, New York, 1980.

[31] A. J. Patti, M. I. Sezan, and A. M. Tekalp, "High-resolution image reconstruction from a low-resolution image sequence in the presence of time-

varying motion blur," in Proceedings of the IEEE International Conference on Image Processing, Austin, TX, 1994, vol. I, pp.343–347.

[32] M. Elad and A. Feuer, "Super-Resolution Reconstruction of an Image," in Proceedings of the 19th IEEE Conference in Israel, Jerusalem, Israel, Nov. 1996, pp. 391–394.

[33] M. Elad and A. Feuer, "Restoration of a Single Superresolution Image from Several Blurred, Noisy, and Undersampled Measured Images," IEEE Transactions on Image Processing, vol. 6, no. 12, pp. 1646–1658, Dec. 1997.

[34] G. Jacquemod, C. Odet, and R. Goutte, "Image resolution enhancement using subpixel camera displacement," Signal Processing, vol. 26, no. 1, pp. 139–146, 1992.

[35] A. T. Erdem, M. I. Sezan, and M. K. Ozkan, "Motion-compensated multiframe wiener restoration of blurred and noisy image sequences," in Proceedings of IEEE International Conference on Acoustics, Speech and Signal Processing, San Francisco, CA, Mar. 1992, vol. 3, pp. 293–296.

[36] R. A. Roberts and C. T. Mullis, Digital Signal Processing, Addison-Wesley, 1987.

[37] S. P. Kim, N. K. Bose, and H. M. Valenzuela, “Recursive reconstruction of high resolution image from noisy undersampled multiframes,” IEEE Transactions on Acoustics, Speech and Signal Processing, vol. 38, no. 6, pp. 1013–1027, 1990.

[38] S. P. Kim and W. Su, “Recursive high-resolution reconstruction of blurred multiframe images,” in Proceedings of the IEEE International Conference on Acoustics Speech and Signal Processing, Toronto, Canada, May 1991, vol. 4, pp. 2977–2980.

[39] S. P. Kim and W.-Y. Su, “Recursive high-resolution reconstruction of blurred multiframe images,” IEEE Transactions on Image Processing, vol. 2, pp. 534–539, Oct. 1993.

[40] A. Papoulis, “Generalized sampling expansion,” IEEE Transactions on Circuits and Systems, vol. 24, no. 11, pp. 652–654, Nov. 1977.

[41] J. L. Brown, “Multichannel sampling of low-pass signals,” IEEE Transactions on Circuits and Systems, vol. 28, no. 2, pp. 101–106, 1981.

[42] S.S. Beuchemin, J.L. Barron, The computation of optical flow, ACM Computing Surveys 27 (1995) 433 –467

[43] S. Borman and R Stevenson, “Spatial resolution enhancement of low-resolution image sequences – a comprehensive review with directions for feature research,” tech. rep., University of Notre Dame, 1998.

[44] R. Kimmel, “Demosaicing: Image reconstruction from color ccd samples,” IEEE Trans. Image Processing, vol. 8, no. 9, pp. 1221 – 1228, Sept. 1999.

[45] Bahadir K. Gunturk, Yucel Altunbasak, and Russell M. Mersereau, “Color plane interpolation using alternating projections,” IEEE Trans. Image Processing, vol. 11, no. 9, pp. 997 – 1013, Sept. 2002.

[46] S. C. Pei and I. K. Tam, “Effective color interpolation in ccd color filter arrays using signal correlation,” IEEE Trans. Image Processing, vol.13, no. 6, pp. 503 – 513, June 2003.

[47] A. Zomet and S. Peleg, "Multi-sensor super resolution," In Proc. of the IEEE Workshop on Applications of Computer Vision, pp. 27- 32, December 2002.

[48] http://software.intel.com/sites/products/documentation/hpc/ipp/ippi/ippi_ch6/ch6_color_models.html, 30.04.2011.

[49] K. Malczewski and R. Stasinski, "Super resolution for multimedia, image and video processing applications," Studies in Computational Intelligence, vol. 231, pp. 171 – 208, 2009.

[50] P. Miklós , "Image Interpolation Techniques," 2nd Serbian-Hungarian Joint Symposium, 2004.

[51] R. G. Keys, "Cubic Convolution Interpolation for Digital Image Processing," IEEE Transactions on Acoustics, Speech, and Signal Processing, vol. ASSP-29, no. 6, pp.1153-1160, December 1981.

[52] B. Horn and B. Schunck, “Determining optical flow,” Artificial Intelligence, no. 17, pp. 185–203, 1981.

[53] B. Zitova and J. Flusser, “Image registration methods: a survey,” Image and Vision Computing vol. 21, pp. 977–1000, 2003.